Spring 2009

# Reliability of resting brain networks using FMRI

Suril Rajeshkumar Gohel
*New Jersey Institute of Technology*

## ABSTRACT

## RELIABILITY OF RESTING STATE BRAIN NETWORKS USING FMRI

**By**
**Suril Rajeshkumar Gohel**

Resting state FMRI studies on human subjects are primarily focused on elaborating effects of resting state brain networks on task induced paradigm and to check consistency of these networks between different groups of populations. Recent studies have shown consistency of RSFC networks within same subjects with intra-site and intra-session variation.

The primary objective of this study was to check consistency of resting state networks between sites and between different groups of people in spite of change in scanning parameters and population. A total of 437 subjects resting state FMRI data from six different sites were collected varying in age group from 21 to 40 years, with scanning parameters varying from site to site. All the data was pre-processed in exactly similar fashion to reduce effects of site variation and to make group comparison feasible.

It was hypothesized that in spite of variation in scanning parameters and population differences, cross-correlation values of time series between 97 ROIs chosen in the brain, should be consistent. To compare resting state connectivity measures, scatter plots of cross-correlation co-efficient between ROIs across sites were used. The investigation demonstrated a strong correlation between cross correlation values for pair of ROIS between sites. These findings suggest reliability and consistency of resting state brain networks between sites.

# RELIABILITY OF RESTING STATE BRAIN NETWORKS USING FMRI

**By**
**Suril Rajeshkumar Gohel**

**A Thesis**
**Submitted to the Faculty of**
**New Jersey Institute of Technology**
**in Partial Fulfillment of the Requirements for the Degree of**
**Master of Science in Biomedical Engineering**

**Department of Biomedical Engineering**

**May 2009**

**APPROVAL PAGE**

**RELIABILITY OF RESTING STATE BRAIN NETWORKS USING FMRI**

**Suril Rajeshkumar Gohel**

5/7/09

Dr. Bharat B. Biswal, Thesis Co-Advisor — Date
Associate Professor of Radiology, UMDNJ

5/7/09

Dr. Tara L. Alvarez, Thesis Co-Advisor — Date
Associate Professor of Biomedical Engineering, NJIT

5/7/09

Dr. Richard A. Foulds, Committee Member — Date
Associate Professor of Biomedical Engineering, NJIT

## BIOGRAPHICAL SKETCH

**Author:** Suril Rajeshkumar Gohel

**Degree:** Master of Science

**Date:** May 2009

**Undergraduate and Graduate Education:**

- Master of Science in Biomedical Engineering,
New Jersey Institute of Technology, Newark, New Jersey, 2009

- Bachelor of Engineering in Biomedical and Instrumentation Engineering,
North Gujarat Hemchandracharya University, Gujarat, India 2007

**Major:** Biomedical Engineering

To my beloved family, you are the reason, motivation and support for what I am today.

"First They Will Ignore You...
Then They will Laugh at You.....
Then They will Fight with You.....
And Then, You win....."
-Mohandas Gandhi

## ACKNOWLEDGMENT

I wish to express my gratitude to Dr. Bharat B. Biswal for his invaluable assistance, support and guidance in course of the research project. Deepest gratitude is also due to the members of the committee Dr. Tara Alvarez and Dr. Richard Foulds for their support and for providing valuable suggestions on the project.

## TABLE OF CONTENTS

## TABLE OF CONTENTS

## (Continued)

## TABLE OF CONTENTS

## (Continued)

**Chapter** **Page**

## LIST OF TABLES

## LIST OF FIGURES

## LIST OF FIGURES
## (Continued)

# CHAPTER 1

# INTRODUCTION

## 1.1 Overview

Functional Magnetic Resonance Imaging (FMRI) due to its high spatial and temporal resolution has become the method of choice for studying brain function both in human and animal models. Advancement in hardware and software has enabled previously used MRI machines to acquire images at a rapid rate thereby enabling fMRI. Since, its first use in 1992, fMRI is currently routinely used in hundreds of clinical scanners to study clinical patients. A number of diverse fields from neuroscience, physiology, biomedical engineering, economics and political science are relying on fMRI to help address several research issues facing their respective field.

In the early years of fMRI, most of the research was done to replicate previously used findings obtained about the brain from other modalities, primarily from Positron Emission Tomography (PET) literature. As a consequence, most of the findings that were obtained using PET have since then been replicated, although with higher spatial and temporal resolution. These studies and findings were very important and have helped to validate several pre-existing hypotheses about involvement of brain regions in different tasks. fMRI has also helped to determine localized effects of task patterns on particular brain regions which were not possible from EEG.

To determine localized regions of the brain, researchers have typically used a stimulus to activate eloquent regions of the brain. Using this methodology, investigators present to the participants, a sensorimotor or cognitive paradigm and compare it with a control paradigm. The objective is then to compare the two conditions (stimulus versus

rest) and find regions that showed the greatest difference between the two. These regions are then labeled as 'activated' regions and are hypothesized to be involved in the stimulus/task presented. Such paradigms have been used to identify and link different brain regions to various tasks including finger tapping, visual tasks, auditory listening, working memory and silent word generation. Such tasks have been used for clinical cases in addition to healthy participants. For a number of clinical populations, fMRI is increasingly being used to map activated brain regions. For example, fMRI is commonly being used as a pre-surgical mapping tool in patients with a brain tumor. Using fMRI, a physician can identify the loss of specific brain function in addition to displacement of the region due to tumor. Similarly, in aging and particularly in Alzheimer's disease, differences in working memory has been used to correlate with the severity of disease and differentiate between dementia and Alzheimer's.

In the beginning years while most of the fMRI research was concentrated on findings regarding eloquent brain regions involved in particular task, some of the researchers concentrated on finding connectivity of different brain regions during a particular task as well as during resting state which can help more to understand physiological structure of working of human brain and to find out details about underlying functional connectivity between different distinct regions of brain apart from overlying anatomical connectivity patterns. Resting state studies, as the name implies are studies where participants are scanned while they are at rest, i.e. in the absence of a task. In this type of study subjects are instructed not to perform any mental or physical task during the scan, they just have to lie down relaxed with their eyes closed but also have to take pre-caution not to fall asleep during studies.

These resting state fMRI studies demonstrated a significant correlation in the sensorimotor cortex, when compared with a time series voxel from the sensorimotor cortex during rest as shown in Figure 1.1a. Few voxels outside the sensorimotor cortex had strong correlation with voxels from the sensorimotor cortex. Because, Friston and colleagues [15] had described, functional connectivity as temporal correlation between physically distant regions, this phenomenon was termed as 'Resting state functional connectivity' (RSFC). Further; these studies showed that these correlations were formed due to the presence of low frequency fluctuations (typically between 0.01 to 0.1 Hz) in BOLD signal representing resting state activity of brain (Figure 1.1b) which then lead to findings about resting state connectivity of different distinct brain regions. These findings eventually helped to determine effects of resting state connectivity on task related connectivity in motor cortex [5].

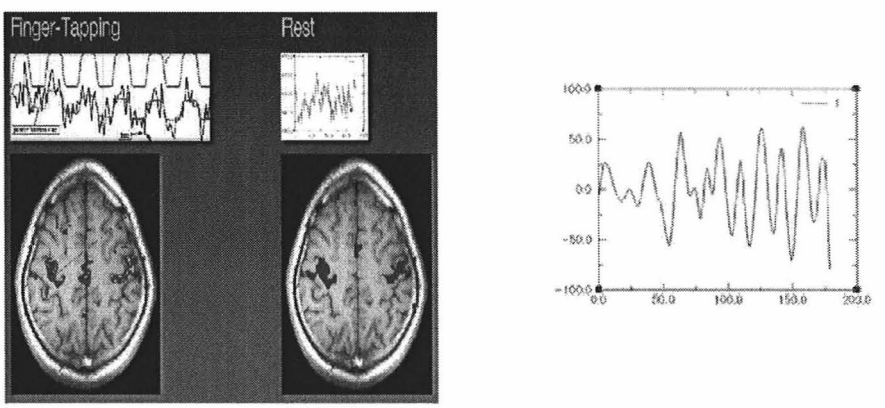


(a) (b)

**Figure 1.1** (a) Extraction of time series from voxel within motor cortex during finger tapping task, (b) Time series of extracted voxels for resting state scan.

Voxel vise correlation of this resting state time series established five resting state brain networks Figure 1.2.

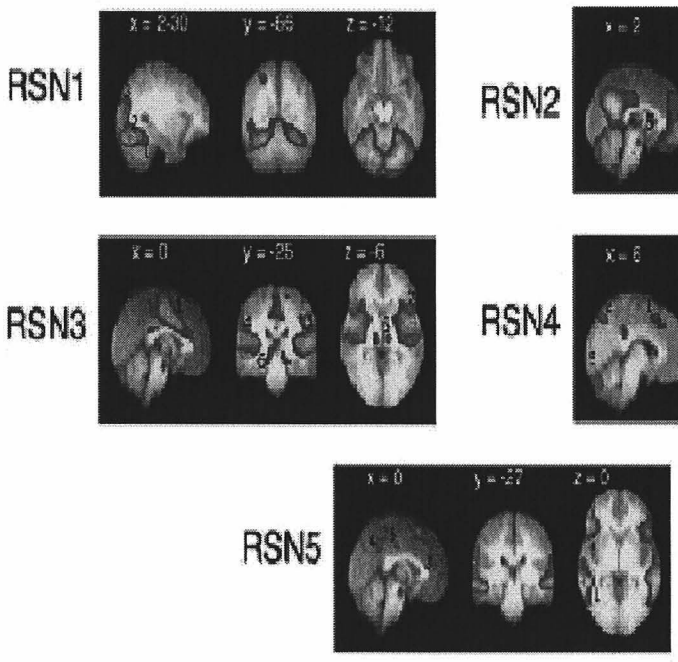


**Figure 1.2** Voxel vise correlation maps for time series extracted from rest scan.

Currently there are many methods being developed to analyze these resting state data available to find connectivity patterns of different distinct brain regions using both region of interest based and voxel wise analysis. Some researchers have used different type of analysis both in the time domain and the frequency domain. As RSFC methods are being more commonly used in the fMRI research, there is a growing need to address the question of robustness of these RSFC maps. In this study, a large number of human subjects obtained from multiple sites using different magnets and imaging parameters were used to study the RSFC between both individual subjects and between groups. Region based (parcellation based) correlation method was used to identify resting state connectivity patterns in brain regions.

## 1.2 Objective

The purpose of present study was to apply region (parcellation units) based correlation methods to check presence and consistency of RSFC between the various brain regions. Resting state fMRI data from different scanning sites was acquired. Each of the dataset was divided in to 97 different Region of Interests defined by Kennedy and colleagues [3]. Cross-correlation matrices were calculated for time series of each pair of these Regions of Interest in order to create a cross-correlation matrix for each of the dataset.

Intra subject and intra site variation were studied for different processing techniques and to check and validate resting state connectivity measures already established.

## 1.3 Background Research

From its development in 1990's fMRI has been widely used to analyze changes in brain's physiology under influence of task pattern and in absence of task pattern. Ogava et al. [4] were the first one to use BOLD (Blood Oxygen Level Dependent) signal to quantify physiological changes occurring in visual motor cortex area during task related activation. Bandettini et al. [1] were one of the first groups to propose and develop basic processing steps for temporal filtering and for correlating each individual voxel from fMRI dataset to the reference time series in order to find out activation for particular task.

Resting state functional connectivity can be described as a method to evaluate brain regions interconnectivity in the absence of explicit task pattern. It was based on discovery by Biswal et al. [5], that low frequency fluctuations in BOLD signal (<0.1 Hz) for anatomically distant regions show a very strong cross-correlation during rest scan.

These variations in BOLD signals are presumed to be representing instantaneous brain function, implicating resting state functional connection between these regions.

Cross-correlation of a time series of a particular brain region "seed regions" with all other brain regions can illuminate which regions is functionally connected with seed region. In general regions that co-activate with seed region tends to have a positive high correlation while regions that become negatively active with positive activation in seed regions tends to have negative correlation value [6,7]. As seed region in general represents any brain region during a particular task activated or resting state fMRI scan, cross-correlation values between time series of these anatomically distant regions provides information about resting state functional connectivity.

There are primarily three sets of seed regions available based on prior work to classify brain in different segments based on anatomical and functional variations. Doesnbach et al. [8] used eight studies comprising a total of 183 scans identified 38 distinct brain regions depending on demonstration of task related activation. They found out two distinct task related networks, former being fronto-parietal network including dorso-lateral prefrontal cortex and intraparietal sulcus while later including dorsal anterior cingulate/medial superior frontal cortex, anterior insula/frontal operculum and anterior prefrontal cortex. Toro et al. [9] used a meta-analysis of 825 neuro-imaging papers to determine 30 regions corresponding to consistent activation throughout the papers. In other studies Kennedy et al. [3] divided brain in 48 different and distinct brain regions to analyze variance in volume for the brain. In a recent study, Shezad et al. [10] used these three studies to check test-retest reliability of default mode network and to study intra subjects and intra session variations.

## 1.4 Outline

The thesis document is divided in following manner. Chapter 2 explains fundamentals of Nuclear Magnetic Resonance, Magnetic Resonance Imaging, Functional Magnetic Resonance Imaging and MRI Instrumentation. Chapter 3 includes data collection and description about basic data analysis steps performed on the dataset for optimal processing with corresponding command implemented. It also includes details about PERL scripts written to implement different pre –processing steps and how a framework was constructed to run all the data sets in a batch process. Chapter 4 describes results of data analysis for the dataset and statistical techniques performed on the results. Chapter 5 discusses the implications of the results and also discusses further lines of work that can be done to extend the present work.

# CHAPTER 2

## FUNDAMENTALS OF MAGNECTIC RESONANCE IMAGING

Magnetic Resonance Imaging is a popular, non invasive imaging modality to study anatomy of brain or for that matter, any region with soft tissue, in detail. Unlike other scanning modalities like CT-Scan or X-ray, it does not use either internal or external radiation and therefore does not create any long time radiation affects on subjects. It is a very useful tool in brain imaging because of three main reasons. First, it provides very high spatial resolution, helpful in imaging minute structures of brain. Second, it provides very good tissue contrast by using different type of pulse sequence which helps a lot in segmentation procedures. Third, as discussed above, is lack of radiation effects, which enables longitudinal studies including different patient populations.

Functional Magnetic Resonance Imaging (fMRI) has evolved as a new imaging technique due to advancement in MRI hardware and software development. fMRI in addition to providing anatomical details of brain with very high spatial resolution also provides temporal information about changes in neuro-physiological activities of brain over a period of time. A similar analogy like digital picture and digital movie can be made between MRI and fMRI. Thus, fMRI help us visualize involvement of brain in various tasks including bilateral finger tapping, auditory text listening, silent word generation, working memory and a host of either stimulus/tasks. fMRI uses changes in intensity of BOLD signal as a representation of brains functional activity. Due to these reasons it has become a very important research tool to evaluate brain regions functions

and inter connections. This chapter describes basic topics and principle related to MRI and FMRI, Nuclear Magnetic Resonance Physics and MRI instrumentation.

## 2.1 Nuclear Magnetic Resonance Physics

Nuclear Magnetic Resonance is a method to observe magnetic properties of different material when subjected to a high density magnetic field. Magnetic properties of materials depend on spin associated with the nuclei of that material which include protons, neutrons and electrons. Spin is defined as natural property like magnetism. Every nuclei posses spin in multiples of +1/2 or -1/2 where (+) specifying positive direction while (–) specifies negative directions. The nucleus of a stable atom consists of spin zero when protons, neutrons and electrons are present in same number because protons and electrons possess spin in different directions. Among all biologically abundant materials hydrogen ion is the most plentiful in human body and magnetic. Water content is largely present throughout the human body, it actually accounts for 70.6% of human grey matter and 84.3% of white matter in human brain, making $^{1}H$ most suitable physiologically. Apart from that $^{1}H$ nucleus has only one proton and no electrons so in this case the spin of the proton can be considered same as spin of nuclei. This nucleus aligns either in parallel or in anti parallel directions with external magnetic field based on their spin directions.

In absence of external magnetic field all of the particles are aligned in random fashion removing effects of each other and making net magnetization vector zero (Figure 2.1a). Under the application of external magnetic field some of the particles aligns them

self in parallel with directions of external magnetic field called lower energy state while some of them aligns them self in anti-parallel with external magnetic field. Now at room temperature level number of particle aligned in parallel with external magnetic field (in

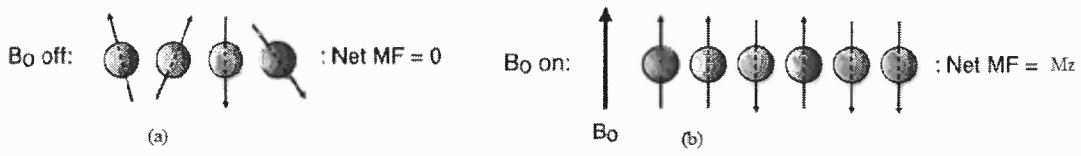


**Figure 2.1** Spin characteristics with and without applied magnetic field. (a) Individual spins aligned in random directions in absence of magnetic field and hence no net spin. (b) Spins aligned in either in the same or opposite direction of the applied magnetism and therefore generating net magnetic moment in the direction of applied magnetic field.

lower energy level) slightly outnumbers number of particles in anti-parallel with external magnetic field(in higher energy level) causing a net magnetization vector to be in parallel with external magnetic field which is basics of MR imaging.(Figure 2.1b). Under application external magnetic field each particle posse's two main properties defined as precession and rotation. Precession of a particle is defined as spinning of particle about axis of an external magnetic field.

The frequency of precession of this particle is called Larmor frequency $\omega_0$ and the relationship between Larmor frequency and magnetic field $B_0$ can be given by following Equation 2.1

$$\omega_0 = \gamma B_0 \qquad \text{or} \qquad f_0 = \gamma B_0 / 2\pi \tag{2.1}$$

In Equation 2.1, $\omega_0$ = Angular precessional Frequency, $\gamma$ = Gyro magnetic ratio, $B_0$= Magnetic Field Strength in Tesla (T) and $f_0$= Precessional Frequency in Hz.

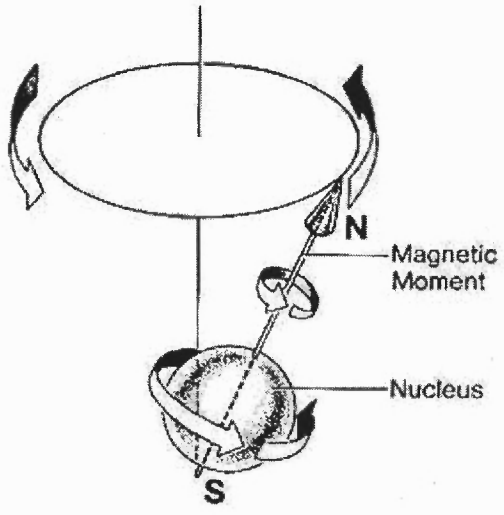


**Figure 2.2** .Precession of a nucleus under the effect of External Magnetic Field $B_0$.

For $^1H$ gyro magnetic ratio is 42.58 MHz/T (Tesla) so for a magnetic field of 1 T precessional frequency would be 42.58 MHz. Apart from precession other phenomenon that occurs is called *rotation.* Rotation of a particle is defined as spinning of particle around its own axis magnetization axis. Figure 2.2 shows rotation and precession of a particle about external magnetic field and its own axis. Conventionally external magnetization is applied in positive Z direction which is perpendicular to X-Y axis. After application of external magnetic field as described before net magnetization vector $M_0$ lies in Z direction which is called longitudinal magnetization vector $M_z$ and after application of high frequency RF pulse net magnetization vector lies in X-Y plane called transverse magnetization vector $M_{xy}$.

## 2.2 Basics of MRI

Magnetic Resonance Imaging (MRI) works on principle of Nuclear Magnetic Resonance. As described before it uses magnetization properties of $^{1}H$ ion, abundantly present throughout the human body.

### 2.2.1 Working of MRI

MRI uses powerful magnets in order to produce high density magnetization field. Without application of magnetic field $B_0$, all $^{1}H$ ions are randomly positioned in human brain producing net magnetization vector of strength zero. Now under the application of external magnetic field $B_0$, some of these ions aligns themselves in parallel with external magnetic field called lower energy state while some of them aligns themselves in anti-parallel with external magnetic field called higher energy state as shown in Figure 2.3 which causes net magnetization vector $M_0$ to be in direction of $B_0$ (commonly referred as Z direction) also known as $M_z$.

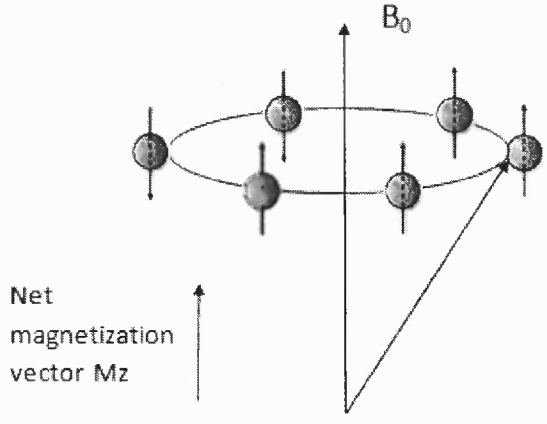


**Figure 2.3** Precessing of Protons around External magnetic field $B_0$ and net magnetization vector Mz.

Under the application of external magnetic field these protons also starts precessing and rotating about external magnetic field Figure 2.3. Precessing direction of these protons are different from each other which cause net magnetization in X-Y direction to be zero. Precession frequencies of these protons are given by Equation 2.1. Change in magnitude and orientation of Mz is necessary to detect Mz .In order to change orientation of this net magnetization vector a high frequency RF pulse is applied having same frequency as precessional frequency in order to create *resonance.*

In general resonance can be defined as tendency of a system to oscillate at its maximum amplitude under the effect of some particular frequency called resonant frequency of that particular system. In MRI, resonance is a very important phenomenon because under the effect of resonance all the energy contained in transmitted RF wave is transferred to precessing protons. In MRI, the resonance frequency of precessing protons is also known as Larmor frequency. If frequency of RF pulse does not match the precessional frequency of protons, resonance cannot occur and in turn net magnetization vector remains in Z direction without change in amplitude or direction. Under the effect of resonance, net magnetization vector $M_0$ flips from Z direction to X-Y direction and tries to align itself with XY direction. This flip angle $\theta$ can be found using Equation 2.2 as follow.

$$\theta = \gamma B_1 t \tag{2.2}$$

Where $\theta$= flip angle, $\gamma$ = Gyro magnetic ratio, $B_1$= External Magnetic Field, t = Duration of RF pulse.

Under the effect of RF pulse protons starts precessing in synchronous with each other producing net magnetization vector in X-Y direction, in addition to this by gaining energy from RF pulse some of the protons in lower energy state goes to higher energy

state, making number of protons in higher energy level almost same as protons in lower energy level. This causes net magnetization in Z direction to be zero and net magnetization in X-Y direction equal to $M_0$. In other words RF pulse causes flipping of net magnetization vector from Z to X-Y direction. From Equation 2.2, it is seen that for a particular material $^1H$ having Gyro magnetic ratio $\gamma$ constant and for a particular scanner having magnetic field density Bo constant, flip angle $\theta$ depends solely on time duration of RF pulse and is in linear proportion with duration of RF pulse. This implies longer duration of RF pulse in order to achieve large flip angles while shorter duration of RF pulse in order to achieve faster imaging.

As described before under the application of RF pulse net magnetization vector flips in X-Y called $M_{xy}$. After the application of RF pulse protons that were precessing in phase with each other starts de-phasing with each other, causing two phenomenon to occur, 1) Decay of $M_{xy}$, net magnetization in X-Y direction and 2) Regeneration of $M_z$, net magnetization vector in Z direction from zero to maximum amplitude.

The decay of $M_{xy}$ (transverse magnetization vector) is defined by transverse relaxation time $T_2$. Transverse relaxation time $T_2$ can be defined as time taken by $M_{xy}$ to reduce to 37% of its original value due to both magnetic field in homogeneities and spin-spin interactions. Relationship between decay of $M_{xy}$ and $T_2$ can be given by following Equation 2.3. Decay of transverse magnetization due to only magnetic field in homogeneity is defined as $T_2^*$ which is generally shorter than $T_2$.

$$M_{xy}(t) = M_0 e^{-t/T2} \tag{2.3}$$

Where $M_{xy}(t)$ = transverse magnetization vector at time t, $M_0$ = net magnetization vector t = instantaneous time t, $T_2$ = Transverse Relaxation time.

The time constant related with regeneration of longitudinal magnetization vector $M_z$ is defined as longitudinal relaxation time $T_1$. It is defined as the time taken by longitudinal magnetization vector $M_z$ to recover to 63% of its original value after application of RF pulse. This time is not same as $T_2$ relaxation time because both are dependent on different properties of material. $T_1$ relaxation time is also known as spin lattice relaxation time because it is the time taken by protons to give out energy to lattice of molecule in order to reach equilibrium stage. Relationship between longitudinal magnetization vector $M_z$ and relaxation time T1 at any instantaneous time t is given by Equation 2.4. Figure 2.4 shows basic curves of $T_1$ relaxation time and $T_2$ relaxation time.

$$M_z(t) = M_0 (1 - e^{-t/T1}) \tag{2.4}$$

Where $M_z$ (t) = longitudinal magnetization vector, $M_0$ = net magnetization vector

$T_1$ = longitudinal relaxation time.

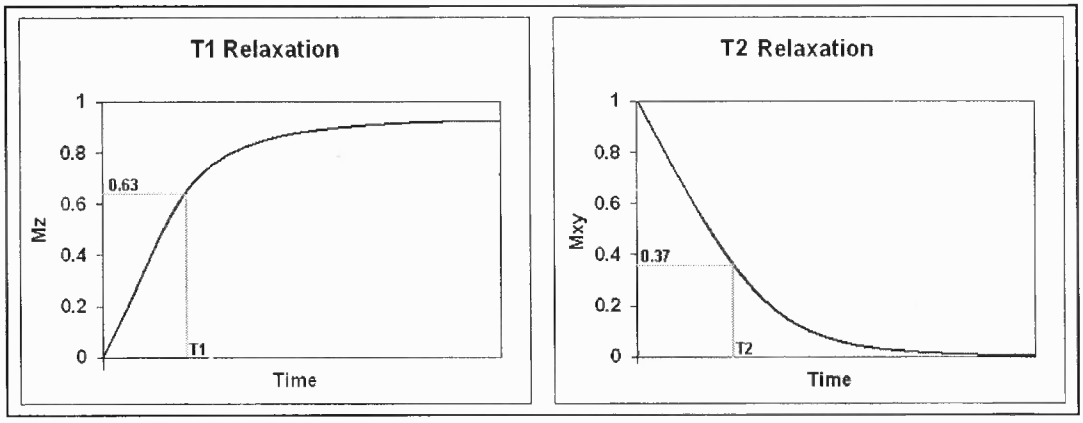


**Figure 2.4** $T_1$ and $T_2$ relaxation time curves.

### 2.2.2 Spatial Encoding

To form an image out of MR signal or to determine specific spectral information, it is very important to relate each MR signal with its location of origin within the sample. This is a very important step regarding image formation and called spatial encoding. *Spatial Encoding* is defined as mapping of a MR signal to its location in brain [11].

In-order to achieve spatial encoding the MRI signal is encoded using different field gradients along successive different axis. These magnetic field gradients are generated using gradient coils which operate in conjunction with magnets to create a linearly increasing or decreasing magnetic field in either direction.

The first step in spatial encoding is called slice-select gradient which as the name specifies, encodes slice information in to MR signal. Initially a gradually varying magnetic field is applied in direction perpendicular to desired slice plane, craniocaudal direction in this case. This gradually varying magnetic field creates planes having different precessional frequency protons perpendicular to it because as described before in Equation 2.1, precessional frequency of proton is dependent upon strength of magnetic field applied. After this a RF pulse having frequency same as precessional frequency of a particular slice is applied in order to create resonance with protons of that slice only. This makes protons in only that slice to resonate and flip in X-Y plane leaving protons in all other slices unaffected.

The second step in spatial encoding is called phase encoding. In this step a magnetic field gradient varying linearly in frequency is applied perpendicular to the slice-selecting gradient for a very brief amount of time before applying a RF pulse. This causes changes in precessional frequency of individual columns for a particular time. Once this

gradient is turned off, it causes precessional frequency of protons in each individual column to be same under the effect of magnetic field provided by main system magnet and there is no difference between precessional frequencies of protons between columns. However, there is a difference between position of protons in the columns that experienced high frequency of precession and columns that experienced relatively low frequency of precession under the effect of phase encoding gradient [11]. Thus after the gradient has been turned off the difference between columns of a particular slice are because of different phase of precession in this columns giving rise to the term phase encoding. In general there are many phase encoding steps required to be performed. In a standard pulse echo sequence number of phase encoding steps needed to be performed is typically same as number of columns in final image.

The third and final step in spatial encoding is defined as frequency encoding. This step works same as phase encoding or slice selecting gradient. This gradient is applied in direction perpendicular to both phase encoding and slice select gradient. Under the effect of this gradient each row in a particular slice is having a different precessional frequency as described with phase encoding gradient. Frequency encoding gradient differs from phase encoding gradient in a way that it is applied only during the time of signal readout or when the RF receiver is ON. Therefore, this gradient is sometimes also referred as readout gradient. Thus at the end of frequency gradient each pixel in an individual column is having same phase difference but is having slightly different precessional frequency.

The MR signal received at the end of this procedures is a mixture of all different frequencies and phase shifts introduced by phase and frequency encoding for a particular

slice selected by slice selection gradient which is than reconstructed using mathematical procedure defined as two Dimensional Fourier Transform (2DFT) [12]. Figure 2.5 shows time cycle for above mentioned different gradients on each individual line with respect to radio frequency pulse.

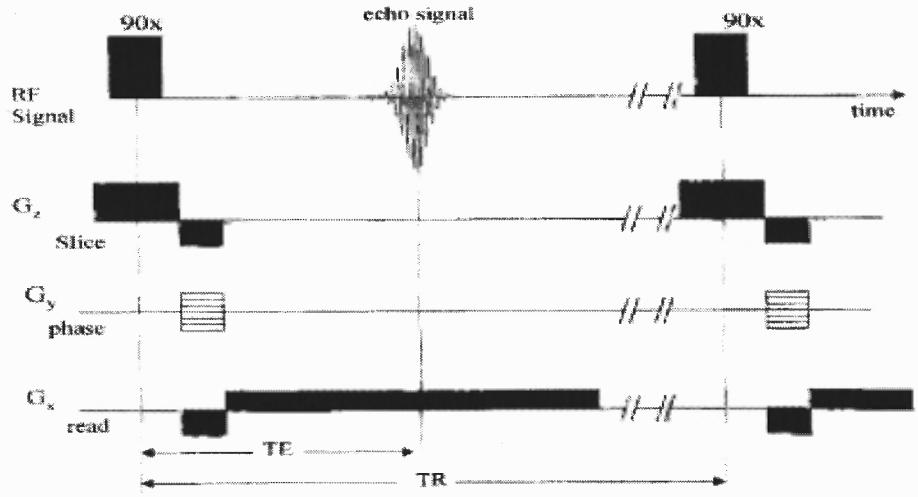


**Figure 2.5** Gradient echo pulse sequence timing diagram.

### 2.2.3 Image Types in MRI

Based on types of contrast involved, MRI images can be divided in primarily in three different sections 1) $T_1$ weighted Images, 2) $T_2$ weighted Images and 3) Proton-Density weighted Images. All three kinds of images differ from each other in terms of tissue contrast and values of TR and TE used to acquire particular type of image. The strength intensity ($S_{SE}$) of a MR signal in a spin-echo sequence at a particular time is given by Equation 2.5.

$$S_{SE} = N(H)\,(1- 2e^{-(TR - TE/2)/T1} + e^{-TR/T1})\, e^{-TE/T2} \qquad (2.5)$$

Where N (H) = Number of spins, TR= Relaxation time, T1= Longitudinal relaxation time, T2= Transverse relaxation time and TE= Echo delay time.

In Equation 2.5 term $(1- 2e^{-(TR - TE/2)/T1} + e^{-TR/T1})$ contains TR ,TE and T1 which indicates exponential growth of MR signal while $e^{-TE/T2}$ term represent TE and T2 which indicates exponential decay in intensity of MR signal.

**2.2.3.1 $T_1$ Weighted Images.** T1 weighted images as name specifies are the types MR images in which the contrast between different tissues is due to difference in longitudinal relaxation time between these different Tissues.

In this type of images shorter relaxation time (TR) and shorter echo delay time (TE) are used to get tissue contrast based on difference of $T_1$ relaxation time. Figure 2.6 shows two different tissue types having different values of $T_1$. Now as time period between two consecutive RF pulses (TR) increases it allows longitudinal magnetization vector enough time to recover to its maximum value. Longer value of Echo delay time allows transverse magnetization vector enough time to decay to zero, the point at which protons are spinning out of phase and in random direction. Shorter value of TR represents large difference in signal intensity due to $T_1$ and also comparatively low difference in signal intensity due to $T_2$. Shorter values of TE represent, receiving the signal comparatively early in order to get less rephasing of protons.

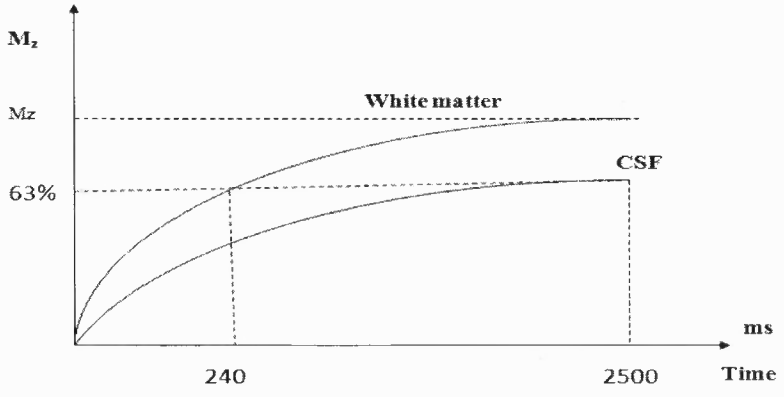


**Figure 2.6** T1 relaxation time curves for CSF and white matter.

Figure 2.7 shows effects of TR on tissue contrast between two tissues. As shown shorter TR (TR1) gives good T1 contrast compare to longer TR (TR2).

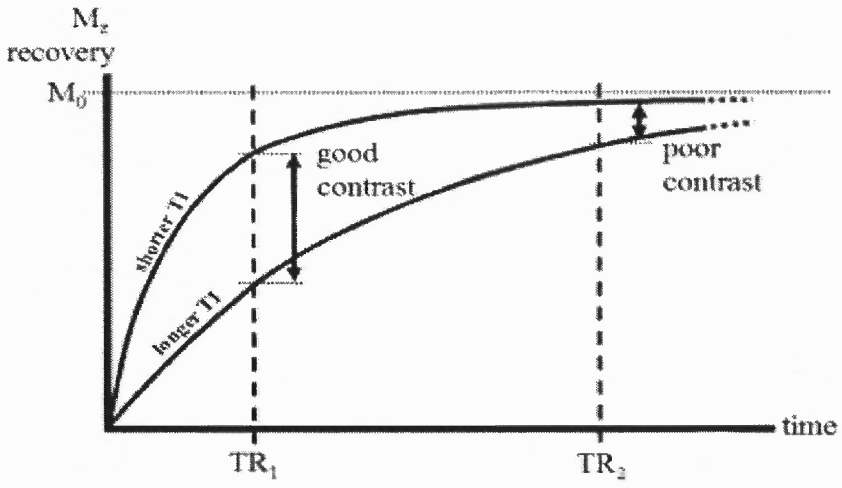


**Figure 2.7** Effects of long and short TR on tissue contrast based on T1.

**2.2.3.2 $T_2$ Weighted Images.** In order to acquire $T_2$ weighted images values of TR and TE are set in such a way to reduce effects of difference of longitudinal relaxation time $T_1$ and to increase effect of difference in transverse relaxation time $T_2$ between tissues.

In order to reduce contrast between two tissue types having similar proton density, value of T1 is kept longer. Longer values of T1 allows longitudinal magnetization vector to recover to its full magnitude. In tissues having similar proton density it is generally same making $T_2$ relaxation time dominant factor in deciding proton density. Figure 2.8 shows effect of longer TE on tissue contrast based on T2 relaxation time.

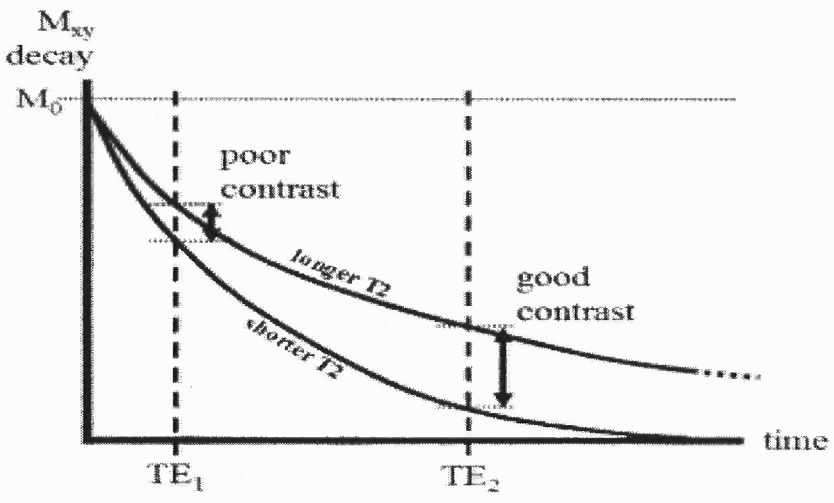


**Figure 2.8** Effects of TE on tissue contrast based on T2.

**2.2.3.3 Proton Density Weighted Images.** As the name suggests, these types of images have tissues contrast based on differences in proton density between two tissue types. This difference in proton density in tissues occurs mainly because of difference in water content in particular tissue.

In this type of imaging relaxation time TR is generally kept larger in order to remove effects of longitudinal relaxation time T1. While echo delay time is kept shorter in order to remove effects of de-phasing and in turn effects of T2. Table 2.1 shows summary of TR and TE required for acquiring particular type of image contrast.

**Table 2.1 Summary of TR and TE used to get Different Tissue Contrasts in MRI**

| Image Type | Relaxation time(TR) | Echo delay time(TE) |
|---|---|---|
| T1 Weighted images | Short | Short |
| T2 Weighted Images | Long | Long or medium |
| Proton density Weighted images | Long | Short |

## 2.3 MR Instrumentation

MR Instrumentation consists of main parts as 1) Main magnets, 2) RF trans-receiver coils 3) Gradient coils, 4) Computer systems.

### 2.3.1 Main magnet

Main magnet is one of the most important parts in MRI instrumentation because characteristics of all other parts are mainly dependent on strength of magnetic field provided by magnet. As described before strength of magnetic field decides precessional frequency of protons which in turn decides RF pulse frequency.

Based on types of magnetization used there are main three types of magnets used in MRI 1) Permanent magnets, 2) Resistive magnets and 3) Super conductive magnets.

Permanent magnets are ferromagnetic types of materials therefore they do not need external excitation to magnetize. These types of magnets are very bulky and cannot generate higher strength of magnetic field. They are cheap and require less maintenance. One of the major disadvantages of this type of magnets is that they cannot be turned off making it very difficult use and requires more precaution to be taken.

Resistive types of magnets works on principle of inductance. It consists of a core around which current carrying coil is wrapped. When the current is flowing through this coil, based on principle of electromagnetic induction it generates electromagnetic field which works as magnetic field for MRI. As the high frequency current is passing through this coil, it generates large amount of heat. For this reason, these types of scanners require a cooling system in order make them work efficiently. Main disadvantage of this type of magnet is that maintenance cost is very high for cooling system and magnetic field generated whose strength typically varies between 0.1T to 0.3T.

Superconducting types of magnets are types of magnets generally used in modern day MRI instrumentation. This type of magnet uses same induction principle as used in Resistive type of magnets but they use phenomenon of super conductance to overcome resistant related difficulties. Super conductance is a phenomenon observed in different types of materials and ceramics under which material posses no resistance to electric current while cooled below certain temperature. In super conducting types of magnets this phenomenon is achieved by submerging the current carrying coils in liquid hydrogen in order to lower temperature which makes this coils works as super conductor. Now as these coils are working as superconductor they show no resistance to electric current reducing heat dissipation related problems. These types of magnets can provide uniformly distributed magnetic field, strength varying from 0.1T to 10T. One of the major disadvantages of these types of magnets is that they are closed structure and may cause problem for claustrophobic patients.

### 2.3.2 RF Coils

Radio frequency coils commonly abbreviated as RF coils are responsible for generation of RF pulse used to flip longitudinal magnetization vector in transverse magnetization vector. Apart from that they also carry out an important function of receiving MR signal back from body.

Based on this two function RF coils should have a uniform excitation throughout the body in order to excite protons throughout the body as well as they should be very sensitive to record a minute changes in MR signal from body. To perform this function there might be two different coils or there might be a single coil performing both functions.

### 2.3.3 Gradient coils

As described before in section 2.2.2, spatial encoding is performed using gradient coils. They are used to provide slice select gradient, phase encoding gradient and frequency encoding gradient.

The main function of gradient coils is to produce linearly varying magnetic field for a particular area. This magnetic field gets added in to the main magnetic field $B_0$ creating a uniformly distributed, linearly varying magnetic field. These linear variations in magnetic field are generated by using a pair of magnetic coils in each spatial direction.

One of the most important criteria while choosing gradient coils is their magnetic field variation provided in mT/m and linearity of magnetic field generate which should be as perfect as possible.

### 2.3.4 Computer system

Controlling of various pulse sequence, gradient coils and main magnets as well as processing of output MRI signal, image reconstruction is done by an internal as well as an external computer system.

Some important criteria to take in to consideration while deciding or choosing a computer system for MR instrumentation are processing speed and ergonomics.

## 2.4 Functional Magnetic Resonance Imaging

FMRI was first proposed by Seigi Ogava et al. [4] for mapping of human brain function. It varies from structural MRI not only in methodology but also in purpose. Structural MRI is used to study structural anatomy of brain. fMRI is used to quantify physiological

changes occurring in brain over a period of time. fMRI has revolutionized brain research in recent years by allowing researchers to locate origins and specific locus of many brain activities which previously was allowed only through approximate correlation of brain anatomy studies of individuals with neurological abnormalities [13].

fMRI has allowed measurement of cerebral blood flow during a particular task within a particular region of brain. fMRI mostly uses Blood Oxygen Level Dependent signal as a measure of changes in physiological activity of brain. It is currently understood that task related activity gives rise to neuronal firing in brain causing higher metabolic activity and thereby lowering the underlying metabolic energy. This creates changes in oxygen level between different tissues giving rise to blood flow and in turn BOLD signal. During a particular fMRI experiment a series of MRI images are acquired over a period of time to record these changes in BOLD signal during both task related as well resting state brain activity.

### 2.4.1 BOLD signal

Past studies have shown a fundamental concept in fMRI that deoxygenated hemoglobin shows paramagnetic properties while oxygenated hemoglobin shows diamagnetic properties under the effect of external magnetic field. Based on prior knowledge of the fact that the presence of paramagnetic substance in blood decrease spin de-phasing and decreases $T2^*$ parameter, Seigi Ogava et al. [4] demonstrated use of this phenomenon to evaluate brain functions based on concentration of deoxygenated hemoglobin present in blood. During any neuronal activity, metabolic activity of brain regions involved increases and metabolic energy decreases which is also denoted as increase in concentration of deoxygenated hemoglobin and decrease in concentration of oxygenated

hemoglobin. This causes a localized increase in blood flow, cerebral blood volume and oxygen supply to these regions.

This increase in blood flow causes decrease in concentration of deoxygenated hemoglobin causing net increase in signal from particular brain region during T2-T2* weighted imaging. Ogava et al. [4] identified this phenomenon of change in brain's functional activity's effect on changes in signal intensity in T2-T2* weighted imaging as a function of concentration of deoxygenated hemoglobin and oxygen in blood as Blood Oxygen Level Dependent signal.

### 2.4.2 Resting State Functional Connectivity

After filtering the fundamental and harmonics of the respiration and heart rates from the data collected using fMRI, BISWAL and colleagues [5] first demonstrated a significant temporal correlation of these low frequency fluctuations between pixels in primary sensorimotor cortex (both intra- and interhemispherically) during rest. These pixels were first identified as active during a finger tapping paradigm. Only a few pixel time courses (<3%) from regions outside the sensorimotor cortex exhibited significant temporal correlation with time courses from pixels within the sensorimotor cortex. Subsequent work by Hampson and Gore has also observed pixels within visual and within auditory cortex [16, 17] that behave similarly; low-frequency fluctuations are correlated within these regions but not outside of them. These studies establish the foundation for resting-state functional connectivity studies using fMRI methodology. Friston et al. [15] had previously defined functional connectivity as the temporal correlation of a neuro-physiological index measured in different brain areas. These studies supported the hypothesis that low-frequency physiological fluctuations constituted such a

neurophysiological index. These intra- and inter-hemispheric correlations among functionally related regions suggest that synchronous fluctuations may be a general cortical phenomenon representing the functional connection of cortical areas.

These results have been replicated and extended by other research groups. Xiong and Fox et al. [18] analyzed resting state fluctuations and identified six areas of the motor system that exhibited significant inter-regional connectivity; primary motor cortex, premotor cortex, secondary somatosensory cortex, anterior cingulate cortex and posterior cingulate. These authors point out that analysis of resting-state SLFF reveals many more functional connections than the usual task-induced activation analysis. They suggest that task-induced activation maps underestimate the size and the number of areas involved in a task and that those are more fully revealed by resting-state fluctuation analysis. Skudlarski and Gore [19] compared fluctuations during three sustained passive stimuli: a pleasant odor, an unpleasant odor and no odor. They reported that odor presentation changed the strength of correlation between some regions in the human cortex, although the effect was weak [19]. Lowe et al. [20] presented subjects with random sequences of either auditory tones or circular symbols and asked subjects to press a button when the auditory tone was heard. In a subsequent scan, the identical sequence was presented but the instructions were to press the button when the visual symbol appeared. The repetition rate was 750 ms. The hypothesis of the experiment was that because all external stimuli were identical between the two scans and the stimulus presentation was fast compared to the sampling rate, any change in correlation between motor, vision, and auditory regions across the two scans should be due to a change in neuronal connectivity mediated by central attention mechanisms. Only three subjects were studied and inter-regional

correlations were small. Nevertheless, it was concluded that the data were significant and consistent with the hypothesis.

Biswal and Hyde [21] studied physiological fluctuations in the motor cortex during a sustained six-minute period of bilateral finger tapping. It was observed in each of four subjects that the magnitude of low-frequency physiological fluctuations was enhanced during continuous finger tapping. In addition, maps produced by analysis of these low frequency fluctuations were coincident with BOLD task-activation maps generated from a block paradigm. These data were consistent with the hypothesis that attention to a prolonged task spontaneously fluctuates. All of the studies reviewed so far (i.e., 19, 20 and 21) have involved sustained motor tasks, sustained attention to changing stimuli or sustained attention to similar stimuli with different response requirements. The interesting hypothesis is that these interregional correlations may reflect effects of a central attentional mechanism upon sensory and motor systems. However, the relatively small effect sizes in these studies make it difficult to assess this hypothesis. The present proposal is to develop experimental methodologies to overcome these technical difficulties to facilitate study of these correlation phenomena.

Low signal to noise ratios in these studies could raise questions about the reliability of these findings. Biswal and colleagues have directly tested the reliability of resting-state functional connectivity maps in fMRI using test-retest analysis. Five resting-state data sets were collected from each subject in addition to bilateral finger tapping to activate the sensorimotor cortex. The reliability of the resting state data sets was obtained using different measures: 1) pixel precision: The ratio of the number of specific activated sensorimotor pixels that passed the threshold in each of the five rest scans to the number

that passed the threshold in at least one of the five rest scans, 2) first-order precision and second-order precision: The numerator of the above ratio is modified to include pixels that passed the threshold in four out of five rest scans and three out of five rest scans. In all subjects it was observed that all five resting state functional connectivity maps had substantial overlap with the corresponding bilateral finger tapping task. While the pixel precision was about 60%, the first-order and second-order precisions were about 70% and 80% respectively. This suggests that there is variability between the resting-state functional connectivity maps. Additional analyses indicate that precision can be increased even more if the activity in pixels immediately adjacent to the active regions (at any of the precision levels) is taken into account.

In recent years there has been a renewed interest in spontaneous fluctuations. Studies have been reported in animals with the laser-Doppler flow (LDF) technique, reflectance oximetry, and FMRI. Hudetz et al. [22] using LDF in the rat cortex, reported that spontaneous fluctuations in the 4-12 cycles-per-minute range were consistently produced when cerebral perfusion was challenged by either systemic or local manipulation. They showed that hypotension, hyperventilation and cerebral artery occlusion substantially modulated the magnitude of the spontaneous fluctuations. These studies challenge current understanding of CBF auto regulation because they suggest the nature of regional CBF may be more dynamic than previously thought.

Improved understanding of RSC could benefit diagnosis of age-related disorders across the lifespan. A study has recently demonstrated altered RSC between hippocampal regions in Alzheimer's disease (AD) patients. Across ten AD patients same group observed significantly fewer resting state correlations between hippocampal regions than

in controls. Moreover, there were minimal differences between AD patients and controls in resting state correlations in visual cortex between these two groups. They had also carried out a study on a diverse group of five patients with Tourette Syndrome (TS). The results of these investigations are reported in a paper in *AJNR* [23], which describes motor task-activation studies and in two abstracts [24, 25] that report on functional connectivity using analysis of physiological fluctuations. Comparisons were made with age- and gender-matched controls. A bilateral finger-tapping paradigm was used for task activation. It is believed that there is a high likelihood, based on these studies that analysis of resting-state physiological fluctuations will contribute to clinical practice.

### 2.4.3 Data collection

For this particular study resting state dataset from six different sites was acquired. Each of the dataset was acquired on different modality of scanner with different number of time points and resolution making results susceptible to effects in change of sites. Table 2.2 shows descriptive measures of dataset by sites.

**Table 2.2 Number of Subjects for Each Site**

| Site Name | Number of subjects |
|---|---|
| State Key National Laboratory, Beijing National University, Beijing, China (China) | 198 |
| Nathan Kline Psychiatric Institute, Orangeburg, NY (Matt) | 42 |
| Medical College of Wisconsin, Milwaukee; WI (MCW) | 65 |
| Child Study Center; New York University, New York (NYU) | 65 |
| Emory University, Atlanta, GA (Georgia) | 28 |
| University of Bangor University, Bangor, UK. (STAN) | 39 |

# CHAPTER 3

# DATA ACQUISITION AND ANALYSIS

Data acquisition and data analysis are the most crucial parts in fMRI experimental setup. The data acquisition parameters provide information regarding the spatial and temporal resolution in addition to the specifics about the experimental design. Data analysis entails the various analytical and statistical procedure used to test the hypothesis. In this chapter, specifics about the data collected and data analysis method has been provided.

## 3.1 Data Acquisition

In this study, 437 healthy subjects with no known neurological or psychiatric diseases were scanned. All subjects were within the ages of 21 and 50 years. The datasets were contributed by six different sites. The six sites included: State Key National Laboratory, Beijing National University, Beijing, China; Nathan Kline Psychiatric Institute, Orangeburg, NY; Child Study Center; New York University, New York; Department of Biophysics, Medical College of Wisconsin, Milwaukee; WI; Department of Psychiatry, Emory University, Atlanta, GA; Department of Psychology, University of Bangor University, Bangor, UK. From each of the sites, 198, 42, 65, 65, 28 and 39 subject data was respectively obtained. All the imaging sites, except Nathan Kline Institute, had a 3 Tesla MRI scanner. Nathan Kline Institute had a 1.5 Tesla MRI scanner equipped with EPI capabilities.

For each of the site two scans were performed: 1) A high resolution MPRAGE image and 2) A fMRI scan covering the whole brain while the subjects were at rest. The

subjects were instructed to keep their eyes open during the rest scan. Very few instructions were given to subjects, other than to refrain from performing cognitive or motor tasks. No further instructions were given.

## 3.2 Data Analysis

Data analysis is one of the most crucial parts of functional MRI experiment. It helps in proving underlying hypothesis for experimenting as well as in preparing datasets for further processing. Data analysis can be divided in two main parts. Former being Pre-processing of the datasets which includes steps to manipulate all datasets in standard formats as well as preparing it for post-processing. Post processing of datasets includes testing hypothesis on the dataset and checking statistical significance of the results.

For this study, data pre-processing consists of steps to detect and correct for motion related signal changes; re sampling the data such that all subjects had the same spatial resolution; realigning all the subject into a standard brain for comparison. A large number of regions were then determined and average time series were extracted from each of the regions from all the subjects and stored for further analysis.

### 3.2.1 Pre-Processing of Datasets

In this experiment all fMRI datasets were from different sites around the world and they were scanned using different scanner modalities. Main purpose for doing pre-processing steps was to process each and every datasets in a particular format in order to make resting state connectivity measures more reliable, independent of individual subjects physiological and anatomical variations as well as independent of scanning parameter

variations. It included processing steps as truncation of time points, de-oblique datasets, changing orientation of datasets, motion correction, brain extraction, de-spiking , spatial smoothing, temporal band pass filtering, de-trending, normalization in to MNI(Montreal Neurological Institute) standard space, extraction of time series for individual ROI mask and averaging of time-series of all the voxels for a ROI mask, in the given order. All of these processing steps were implemented using three software packages AFNI, FSL and MATLAB 7.0 explained in detail. To implement this pre-processing steps a PERL script was written in which each of the pre-processing step was defined by a unique User Defined Function.

**3.2.1.1 Truncation of Time Points.** First pre-processing step was truncating first five time points from each and every dataset. While scanning of fMRI subjects generally first five time points are discarded to remove relaxation due to T1 effects. This step was performed using 3dcopy command of AFNI software package. Following is the syntax of command used in the algorithm.

3dcopy rest+orig [5..110] trunk_rest (3.1)

This command will take an input dataset labeled as rest+orig and will take time points from the fifth time till the $110^{th}$ time point.

**3.2.1.2 De-Oblique Dataset.** For FMRI datasets EPI datasets were generally acquired in oblique pattern while anatomical datasets are generally acquired in cardinal space. Because, various datasets were acquired using different imaging parameters, all the data sets were transformed into orthogonal space, where the images when observed from the three axis coordinate system would lie in axial, sagittal and coronal plane. While standardizing EPI dataset to a standard MNI brain template, it is necessary that this EPI

dataset and anatomical dataset corresponds to each other which can be done by either applying De-oblique operation to EPI datasets or by applying oblique operation to anatomical dataset. This was implemented by replacing transformation matrix in header of EPI dataset with cardinal matrix. Following options were used to implement this command in Equation 3.2.

3drefit –deoblique –prefix DO_rest trunk_rest+orig. (3.2)

Where –deoblique represents replacing of transformation matrix with cardinal matrix, DO_rest+orig.BRIK/HEAD is output dataset name while trunk_rest+orig is input to the function which is output of the preprocessing step truncation of time series.

**3.2.1.3 Reorientation of fMRI Dataset.** This experiment consists of datasets from different and consequently acquisition parameters varied from site to site in many ways including the number of volumes collected, the spatial resolution and orientation of brain in data acquired. The orientation information is stored in the header file corresponding to the image. This information is typically coded into one three letter word as:

1. **R**ight – **L**eft, Letter **R** or Letter **L** represents whether X increases from Right to Left or X increases from Left to Right respectively,

2. **P**osterior – **A**nterior, Letter **P** or Letter **I** represents whether Y increases from Posterior side of subject to Anterior side of subject or Y increases from Anterior side to Posterior side respectively and

3. **I**nferior – **S**uperior, Here Letter **I** represents that Z direction (slices of FMRI dataset) are represented from Inferior to superior while letter S represents that slices are ordered from Superior to Inferior.

It is of primary importance that all the datasets are aligned in a particular order so that any random voxels chosen from all the dataset refers to a particular part of human

brain. For this reason all the fMRI datasets were aligned in to RPI (Right to Left, Posterior to Anterior and Inferior to Superior) format. This step also helped facilitated the normalizing all datasets in to standard MNI template which was accomplished using FSL software package. To implement this processing step 3dresample command from AFNI package was used as shown in Equation 3.3.

3dresample –orient RPI –prefix reor_rest DO_rest+orig (3.3)

In this command RPI represents final orientation of the desired dataset,-prefix represents name of output datasets which in this case will be reor_rest+orig.BRIK/HEAD and input is DO_rest+orig which is deobliqued dataset.

**3.2.1.4 Spatial Realignment (Motion Correction).** During a single fMRI data acquisition, a large number of sequential images are obtained at very fast rate, typically 32 images every two seconds. This is acquired continuously for about five minutes. Although, subjects are instructed not to move their head and to restrict head motion as much as possible, even motivated subjects move their head by a few mms. The main effect of this head motion during a particular fMRI scan is that same voxel represents different location of brain over a period of time. This causes a change in signal intensity and may not be uniform throughout the whole brain and is in direct contrast with the basic assumption for fMRI time series that each voxel in fMRI dataset represents same location in brain over a period of time.

For example, when a particular voxel having original position in low activity region of brain moves to region nearby having comparatively higher activity in fMRI image due to head motion, it appears over a period of time that the fMRI signal activity for that voxel has increased or changed while in reality signal from that particular brain

region hasn't changed (Figure 3.1). The fMRI signal change seen is the result of head motion can give rise to two potential consequences in further processing of fMRI data 1) If the data collected is task data which is than to be correlated with some reference time series, it can give rise to higher value of correlation or false correlation for that particular voxel and can change statistical inference and 2)Even with resting state fMRI it can give rise to a lot of noise in fMRI time series which in turn can affect cross-correlation measures done to check brain regions interconnectivity and statistical inferences.

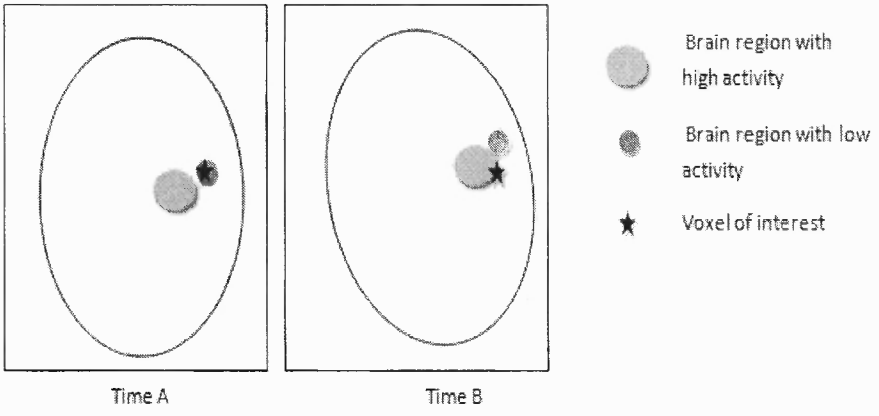


**Figure 3.1** Effect of head motion between time A and Time B on location of a particular voxel.

The removal of head motion is done on individual basis for each subject, for each run and it is called spatial realignment or alternatively motion correction in general terms. In this step first a reference brain volume is taken and than all other brain volumes are realigned corresponding to this reference brain volume. For this realignment a minimization algorithm for least square difference of volumes in the time series and reference volumes is used. That simply means that for each volume squared difference between reference volume and that particular volume in time series is minimized. The

new value of realigned fMRI voxel is determined by interpolating fMRI signal values from neighboring voxel.

Choosing a reference volume is subjective because if the volume chosen as reference contains motion whole realignment process may become unstable. Typically, a reference volume is chosen from first few time points of particular scan under the assumption that during first few time points' motion is less which in general case is true.

For this study mean volume of dataset was taken as a reference volume to remove effects of variation of different number of time points for different scan between sites. 3dvolreg command from AFNI software was used to implement spatial realignment and 3dTstat command from same software was used to calculate mean volume of the dataset as shown in Equation 3.4a and 3.4b.

3dTstat -mean –prefix mean_MC_rest reor_rest+orig. (3.4a)

Where –mean represents averaging operation, -prefix is output name which in this case is mean_MC_rest+orig.BRIK/HEAD and input to the command is reor_rest+orig.

3dvolreg -fourier –base mean_MC_rest+orig. –prefix MC_rest (3.4b)

Where 3dvolreg specifies that processing to be performed is spatial realignment by taking reference volume as mean_MC_rest+orig and using interpolation techniques as Fourier interpolation. Input is reoriented dataset from previous processing steps and output dataset is MC_rest+orig.BRIK/HEAD.

**3.2.1.5 Brain Extraction.** In fMRI inhomogeneities in magnetic field causes the fMRI signal to decay over a period of time. Although many efforts are taken to make magnetic field as homogeneous as possible, there are some small local magnetic inhomogeneities that are still present. These inhomogeneities cause artifacts in the fMRI

image particularly on tissue-brain and tissue-bone boundaries which are also known as susceptibility artifacts. These artifacts can be generally seen as an aura around brain region which sometime affects process of standardizing individual brain with standard MNI template brain.

Process of removing these artifacts from fMRI data is called brain extraction while for anatomical images it is sometimes also referred as skull stripping because of skull present in the anatomical data. For EPI datasets, brain extraction was performed using 3dAutomask command from AFNI toolbox. This command will generate a mask of brain from input dataset which in turn will be multiplied by the dataset itself to extract brain from the dataset. To multiply mask generated by 3dAutomask command with the FMRI dataset a command called 3dcalc was used from AFNI software as shown in Equation 3.5a and 3.5b.

3dAutomask –dilate 1 –prefix mask_rest MC_rest+orig. (3.5a)

Output mask name will be mask_rest+orig.BRIK/HEAD while input dataset is MC_rest+orig. Option -dilate 1 specified to extend brain boundaries of mask by one after creating mask because by default command 3dAutomask shrinks brain by one voxel to provide better brain extraction.

3dcalc –a mask_rest+orig –b MC_rest+orig.

–expr 'a*b' –prefix masked_rest (3.5b)

This command specifies two input datasets defined by variable "a" which represent mask created by 3dAutomask command and variable "b" represents motion corrected dataset from which brain is needed to be extracted. Option –expr specifies mathematical operation needed to be performed on input dataset (multiplication in this

case specified by 'a*b') and storing result in output dataset as masked_rest+orig.BRIK/HEAD specified by option –prefix.

**3.2.1.6 De-Spiking of Voxel Time Series.** The primary purpose of De-spiking is to remove high spikes in the dataset which are caused either due to large fMRI signal variation or head motion which were still not removed from motion correction.

Head motion produces spikes in the edges of brain represented in time-series of voxel around edges in the brain. Now these spikes might affect correlation results as explained previously as well as these spikes might also elevate mean value of fMRI time series which can affect process of removing linear trend and might as well change percentage signal change and statistical inferences based on this. To perform this operation 3dDespike command from AFNI was used as shown in Equation 3.6.

3dDespike –ssave spikinesss_rest.1D –prefix ds_rest masked_rest+orig (3.6)

Where input is masked FMRI dataset names masked_rest+orig, output dataset is despiked_rest+orig.BRIK/HEAD. This command also saves a file named spikiness_rest.1D which contains spikes information about each voxels in the dataset.

**3.2.1.7 Spatial Smoothing.** Spatial smoothing is one of the most important steps used in fMRI pre processing. Spatial smoothing reduces the presence of random noise and improves signal to noise ratio which in turn helps improve the signal quality. While spatial smoothing improves the SNR, the spatial resolution is reduced. For this reason choosing smoothing criteria is a very important factor to decide in order to obtain balance between SNR and spatial resolution. In this study, spatial smoothing was implemented using a three dimensional Gaussian kernel. To implement this function fslmaths command from FSL software was used. Spatial smoothing on NIFTI converted de-

spiked dataset which is now called ds_rest.nii.gz was performed as shown in Equation 3.7a.

fslmaths ds_rest.nii.gz –kernel gauss 2.55 –fmean –mask mask_rest.nii.gz smooth_rest.nii.gz (3.7a)

This command specifies to perform smoothing operation with Gaussian kernel of size 2.55 sigma which is same as Gaussian kernel of size 6 FWHM and store output dataset as smooth_rest.nii.gz.

After this the next step was global intensity normalization which was done by dividing dataset by global mean and then multiplying it by 10000 using following command in fslmaths.

fslmaths smooth_rest.nii.gz -ing 10000 gmean_rest.nii.gz -odt float (3.7b)

This specifies input dataset name as smooth_rest.nii.gz, mathematical operation needed to be performed as –ing specifying intensity normalization with global mean and storing output in dataset name gmean_rest.nii.gz in float.

After performing Spatial smoothing and intensity normalization, output dataset named gmean_rest.nii.gz is converted in to AFNI format with 3dcopy command used in following context.

3dcopy gmean_rest.nii.gz smooth_rest (3.7c)

Which takes input as 4D NIFTI dataset named gmean_rest.nii.gz which is output of previous processing step and converts them in to 4D AFNI files named smooth_rest+orig.BRIK/HEAD.

**3.2.1.8 Temporal Filtering of Voxel Time Series.** Temporal Filtering is one of the most important pre-processing steps while dealing with resting state FMRI datasets due to frequency nature of resting state fMRI signals. As spatial smoothing of fMRI dataset improves Signal to Noise Ratio (SNR), temporal filtering can also help in improving SNR as well as for signal separation. Temporal filtering included filtering of individual time series of each fMRI voxels in order to separate signal from noise. In this case band-pass filtering for a frequency band of 0.005 to 0.1 Hz which means having a low cutoff frequency of 0.1 Hz and having high cutoff frequency of 0.005 Hz was performed on each dataset.

The reason this particular frequency band was used is because this particular frequency band represents low frequency fluctuation in fMRI signal in resting state as reported by Biswal et al. [5]. To implement this filtering option 3dFourier command from AFNI tool box was used with following options.

3dFourier –lowpass 0.1 –highpass 0.005 –prefix filt_rest –retrend smooth_rest+orig.BRIK (3.8)

Where output dataset filt_rest+orig.BRIK/HEAD is created by applying band pass filtering operation having low cutoff frequency of 0.1 Hz and High cutoff frequency of 0.005Hz on input dataset named smooth_rest+orig.BRIK/HEAD. Here -retrend option specifies that any mean or linear trend in the dataset will be removed prior to filtering and then will be added back after filtering.

**3.2.1.9 Linear Trend Removal (De-trending).** The inherent nature of fMRI data of having a very low Signal to Noise Ratio makes removal of low frequency signal intensity drift from fMRI data an important processing step particularly while dealing with brain regions having very low activation and for resting state fMRI data in general. Two main sources of linear drift are noise from MR scanner and aliasing of fMRI data with physiological pulses.

In this pre-processing step, removal of linear trend was implemented using 3dDetrend command of AFNI software which uses removal of least square components from each voxel time series. Implementation of linear trend removal also includes adding mean back in to de-trended dataset in order to make percentage signal change constant.

De-trending of FMRI datasets was performed in following three steps using commands available from AFNI software. First step is calculating mean of the input dataset using 3dTstat command available from AFNI as shown in Equation 3.9a.

3dTstat –mean –prefix mean_rest filt_rest+orig (3.9a)

This command uses function 3dTstat to calculate mean of the input dataset filt_rest+orig.BRIK/HEAD and output dataset named mean_rest+orig.BRIK/HEAD.

Second step was removal of linear trend using command 3dDetrend from AFNI software in following context.

3dDetrend –prefix dt_rest –polort 2 filt_rest+orig. (3.9b)

This function specifies de-trending performed on dataset named filt_rest+orig using Legendre polynomials of order up to order two specified by option -polort 2. Now this option removes mean of the dataset also making every time series of fMRI voxel at same base level which changes percentage signal change for a particular signal. For this

reason at the end of de-trending it is necessary to add mean back in to the signal making % signal change constant. This step was implemented using 3dcalc command from AFNI software.

3dcalc –a dt_rest+orig –b mean_rest+orig –expr 'a+b' –prefix rd_rest (3.9c)

Which takes input 'a' as de-trended data called dt_rest+orig.BRIK/HEAD and input 'b' as mean of the dataset before de-trending called mean_rest+orig.BRIK/HEAD, takes summation of this two datasets explained by option 'a+b' and stores data in dataset named rd_rest+orig.BRIK.HEAD.

**3.2.1.10 Spatial Normalization and Co-Registration.** During a particular FMRI experiment, dataset includes data from several different subjects rather than a single subject several times. These subject brain scans differ from each other in terms of orientation, size and shape of brain from subject to subject making intra-subject comparison difficult. For this reason size, shape and orientation of each and every human brain is changed to match that of standard human brain. One of the main reasons for doing this is to make a particular FMRI voxel represent same anatomical region of brain between different subjects or runs. Another reason for doing this is that it makes all scanned brain volumes same which makes number of voxels for each dataset same, making statistical comparison and group analysis of the dataset easy. This process of standardizing each subject's individual brains to a standard brain is called spatial normalization.

In this experiment this process is done in two parts, one of them being spatial co-registration and other one is spatial normalization. Standardization of each individuals EPI brain scan with that particular individuals high resolution anatomical brain scan is

called spatial co-registration. Main purpose of this procedure is to make comparison between different modalities of scanning easy. In this experiment main purpose of doing spatial co-registration was to use high resolution details of anatomical dataset to transform very low resolution EPI dataset to standard brain. Choosing a standard can be a very important factor regarding data-storage and computational time.

For this experiment a standard MNI brain template with voxel size of 2mm X 2mm X 2 mm was used. Next step was implementation of flirt command to derive transformation matrix from anatomical brain to standard brain as described below in Equation 3.10a.

Flirt -in mprage.nii.gz –ref avg152T1_brain.nii.gz -omat rest_mni1.mat mat -bins 256 -cost corratio -searchrx -90 90 -searchry -90 90 -searchrz -90 90 -dof 12 (3.10a)

Equation 3.10a specifies, taking input as mprage.nii.gz (High resolution Anatomical dataset), reference as avg152T1_brain.nii.gz which is standard brain dataset in MNI format derived from averaging 152 different subject. Options –omat rest_mni1.mat specifies that output transformation matrix should be stored in rest_mni1.mat, -cost specifies cost function to use while performing transformation which is set to correlation ratio in this case and –dof 12 specifies to use 12 degree of affine transformation for normalization.

Next step is creating transformation matrix for spatial co-registration which is normalizing EPI brain to Anatomical brain in native space using rigid-body transformation of six Degree of Freedom. Input to this function was de-spiked EPI dataset in order to use all anatomical information available from EPI dataset.

Flirt –in cp_rest.nii.gz –ref mprage.nii.gz -omat rest_mni2.mat mat -bins 256 -cost corratio -searchrx -90 90 -searchry -90 90 -searchrz -90 90 -dof 6. (3.10b)

This saves transformation matrix in rest_mni2.mat created using rigid body transformation with six Degree of Freedom. After creating two transformation matrices named rest_mni1.mat and rest_mni2.mat, next step is to combine this two transformation matrices to create a third transformation matrix which than has information to normalize EPI dataset to standard MNI rain dataset. This was performed by concatenating this two transformation matrices using following command specified in Equation (3.10c) in FSL.

convert_xfm -concat rest_mni1.mat -omat rest_mni.mat rest_mni2.mat (3.10c)

Final step in spatial normalization is to apply this transformation information to standardize EPI dataset to MNI standard brain dataset.

Flirt –in rd_rest.nii.gz –ref avg152T1_brain.nii.gz –out rest_mni –applyxfm -init rest_mni.mat -interp trilinear. (3.10d)

This specifies input dataset as rd_rest.nii.gz, transformation matrix to use as rest_mni.mat and interpolation method to use as tri-linear which is default in this case. Output dataset will be stored as rest_mni.nii.gz which is EPI dataset normalized in to standard brain having voxels size of 2mm X 2 mm X 2 mm.

**3.2.1.11 Extraction of Time Series.** Extraction of time series from standardized EPI dataset was next pre-processing step. In this experiment brain was divided in 110 different ROIs (Region of Interests) specified by Kennedy et al. [3]. A 50% probability mask was drawn for each of the ROI specified on standard MNI brain template. These masks were used to extract time series from standardized EPI brain dataset derived from previous processing step. For each mask time series of voxels falling

in particular mask were extracted and stored in different file for each of the mask. Figure 3.2 shows four sample ROI masks used overlaid on standard MNI brain template.

To extract time series from each mask 3dmaskdump command was used from AFNI software in following context.

3dmaskdump –mask "maskname" -o "outputfile"

–noijk rd_restmninew+tlrc. (3.11)

Where maskname specifies the name of the dataset to be used a mask, –o specifies name of the output file which will be having individual time series for each voxel in that mask, –noijk specifies not to give out x, y, z co-ordinates for each voxel in the mask and input dataset name is rd_restmninew+tlrc.BRIK/HEAD. Output file contains number of rows equal to number of voxels in the particular mask while columns representing time points for that particular dataset which ranges from 110 to 470 based on site.

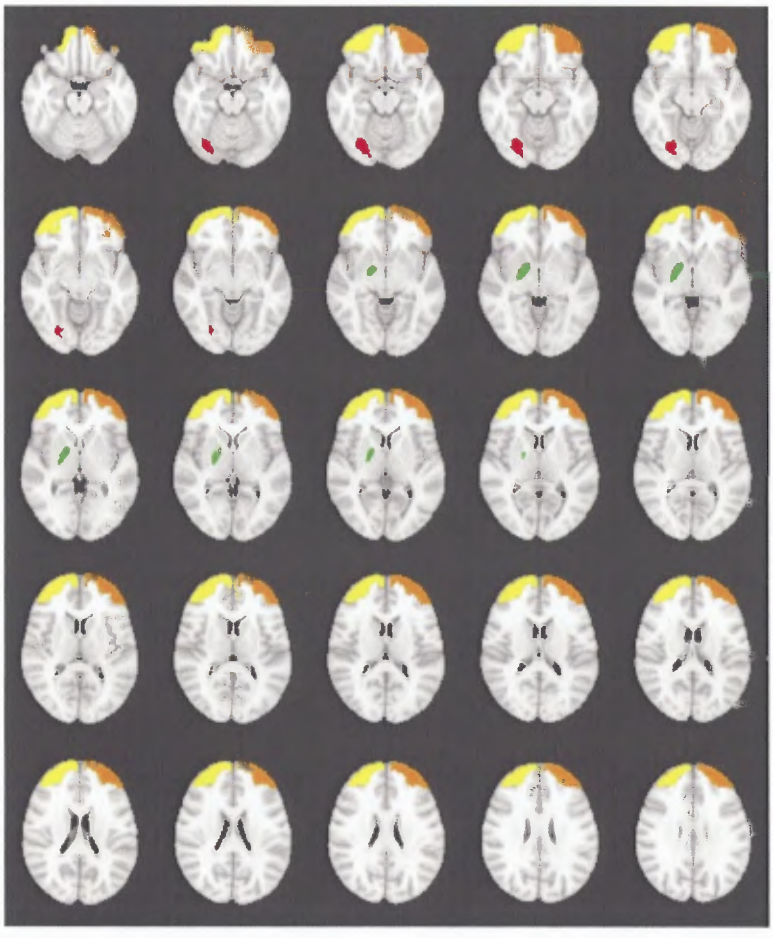

**Figure 3.2** Four sample ROI masks used overlaid on MNI standard brain template Output file contains rows equal to number of voxels in the mask while columns.

**3.2.1.12 Averaging of Extracted Time Series.** Every ROI mask used for time series extraction varied in size and shape depending on anatomical part of brain it represented. Thus each ROI have different number of voxels. For this reason, an average time series was obtained for each ROI by averaging all the time series in that ROI. For each subject, a new matrix was created whose 110 rows represented mean time series of each of different Region of Interest from both left and right hemisphere of EPI dataset. In this dataset first 55 rows represented mean time series from Region of Interests belonging to left hemisphere while later representing mean time series from

Regions of Interest belonging to right hemisphere in the brain. Output of this program was a .mat file which named rest_lr_kenedy.mat which while loaded in MATLAB workspace represented mean time series for each Region of Interest as individual rows while columns representing different time points or change in FMRI signal intensity over a time course.

### 3.2.2 Post-Processing of Datasets

Post-processing steps for this dataset consists of calculating pair wise correlation for each individual set of Regions of Interests. As noted before, post processing of fMRI dataset generally includes hypothesis testing on the dataset and checking statistical significance of results on the dataset. In this experiment our hypothesis was that consistent resting state network would be observed across all the subjects and this consistent correlation pattern found represented, inherent connectivity.

**3.2.2.1 Cross Correlation.** Correlation is a simple statistical procedure to measure degree of similarity between two different sets of data. Value of correlation between two different datasets ranges from -1 to 1 where 1 represents that both the datasets are identical and there is virtually no different between these two types of data. A zero represents that both dataset has no similarities in between. Negative values of correlation between two datasets represents that they are out of phase with each other. In general value of correlation between two different signals is a measure of linear dependence of these two signals on each other. Correlation was used as one of the measure to check dependency of time series from each ROI time series with every other ROI time series. Pair wise correlation coefficient was calculated using corr2 function available through MATLAB for each pair of time series for each ROI. Higher values of

correlation between any of these two regions implies to higher order of similarity between these two signals. These signals from two different ROIs of brain consist of very low frequency signal (0.005 – 0.1 Hz) after pre-processing, which mainly represents activity of these two brain regions during resting state.

# CHAPTER 4

# RESULTS AND DISCUSSION

In this section results obtained after both pre-processing and post processing of data are reported and elaborated. As described before head motion is a primary cause of noise induced in fMRI signal. Apart from causing noise in the signal received, it can also lead to false activation as discussed before in section 3.2.1.4. For this reasons it is of utmost important to remove data from the subjects having too much head motion. To remove the effects of head motion spatial realignment was performed on each of the input dataset. But due to nature of the study, (resting state study) less head motion was expected and was observed across subjects for this reason none of the subjects were discarded from the studies due to head motion. Apart from this as mean of time series of voxels contained in each individual ROI was taken. Effect of very little head motion can be considered negligible on mean time series of all the ROI voxels.

fMRI data used in this study was acquired from six different sites spanning across three continents. One of the preliminary differences between these data within each site was Field of View taken for each subject scan. Due to variation of FOV between sites and difference of brain size between subjects, spatially normalized data from each site were not identical but were having a very little subject to subject variation. From a total pool of 437 subjects acquired less than 7% of data was discarded due to this reason.

All the ROI masks chosen were drawn on standard MNI brain template of size 2mm X 2mm X 2mm and were not locally drawn for each subject. Now due to variation in brain size between subjects, some of the ROI masks representing brain regions near the

edge of the brain were lying outside the normalized brain for < 10% of total subjects while other ROI masks were present and were at particular location in normalized brain. As those ROIs were outside the brain region; time series for this ROI masks contained zeros. Auto correlation of this time series gives value of 'Nan'(Not a number value) and cross correlation value of this time series give value of zero due to no similarity with time series of any other brain regions. These values can give rise to faulty statistical inferences and also decrease reliability of resting state networks measures. For this reason data from 13 out of 110 ROIs were discarded from each subject in order to make resting state network measures more robust.

As described before in section 3.2.2.1 cross –correlation matrix for a set of Region of Interests show cross –correlation values of mean time series of each individual ROI mask with time series of all other ROI mask. For all 413 subjects studied, cross-correlation matrix for mean time series of 97 different ROIs was created. Figure 4.1 and Figure 4.2 shows cross-correlation matrix for subject 5 and subject 201, respectively.

Each of the pixel in Figure 4.1 and 4.2 shows cross correlation value between mean time series of region of interest defined by x and y co-ordinate of that particular pixel. For example value of 0.7539 at co-ordinates (23, 47) represents cross-correlation value between ROI number 23 and ROI number 47. For this particular reason cross – correlation matrix or image is symmetrical about its main diagonal because correlation between region 23 and 47 (23, 47) or between region 47 and region 23(47, 23) is same.

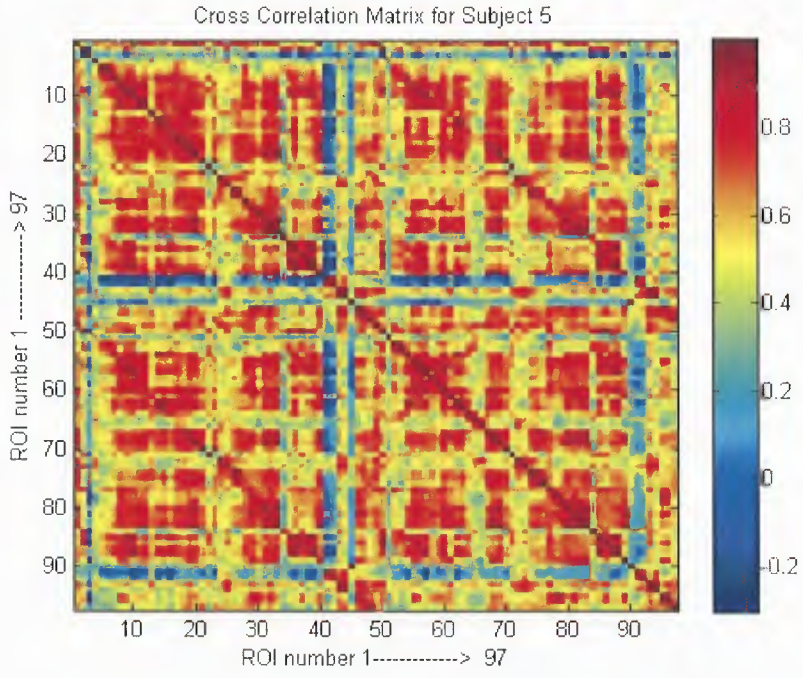


**Figure 4.1** Cross Correlation matrix for subject number 5.

.

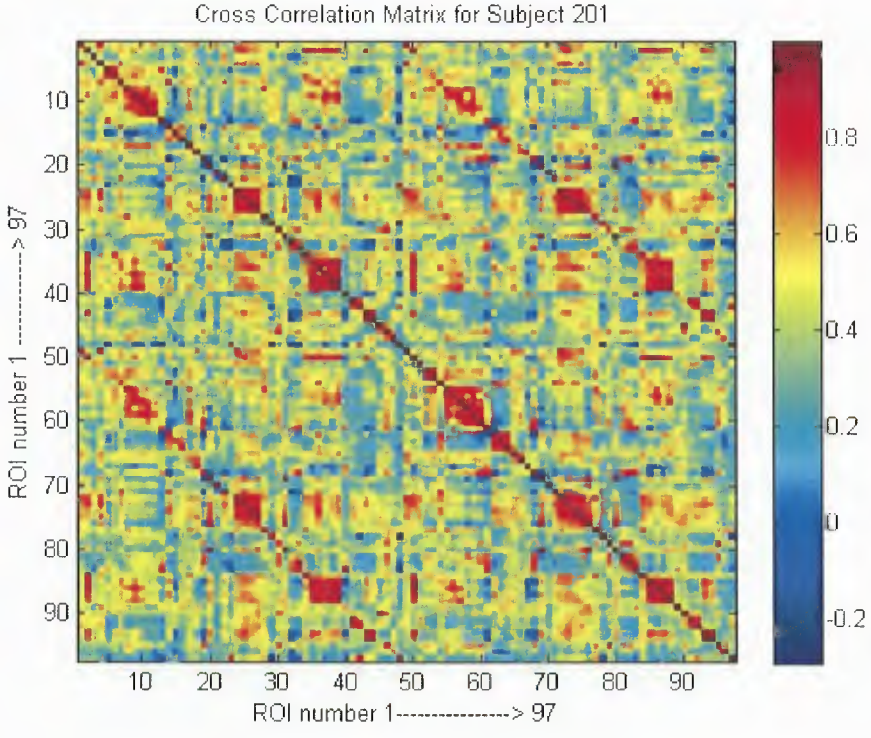


**Figure 4.2** Cross Correlation Matrix for subject number 201.

As seen from Figure 4.1 and 4.2 diagonal of cross correlation matrix is having a value of one because it represents cross-correlation of an individual ROI time series with itself.

To remove effects of variation in number of subjects between different sites mean of cross-correlation matrix for each site was taken as well as a mean cross correlation matrix across subjects of all sites was taken to compare variation in mean of cross correlation of each ROI pair across sites. The diagonal of cross-correlation matrix which is having value of one in every subject across all the sites can give rise to false assumption of similarity between two sites. To avoid effects of diagonal on intra-site comparison, each individual diagonal value representing cross –correlation value of a ROI with itself was replaced by mean cross correlation value of that ROI across cross-correlation matrix.

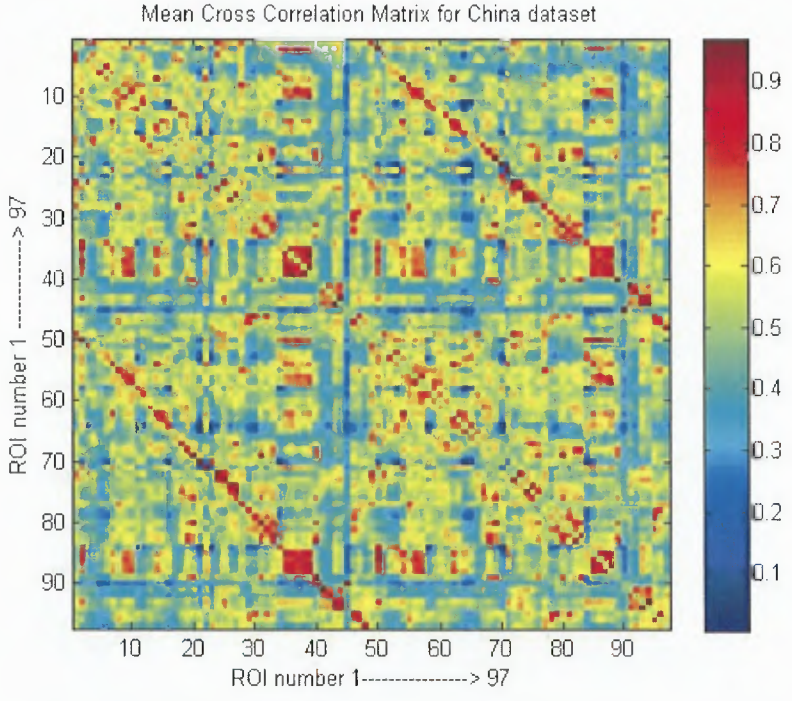


**Figure 4.3** Mean Cross-correlation matrix for China dataset.

Figure 4.3 and Figure 4.4 shows mean cross-correlation matrix across all subjects of china dataset and across subjects from all sites respectively. As discussed before each value in main diagonal of the matrix was replaced by mean cross-correlation value of individual ROI across cross-correlation matrix.

Visual similarities between mean cross-correlation matrix of individual sites as well as between sites and mean across all subjects can be seen confirming hypothesis of reliability of resting state brain networks between different sites.

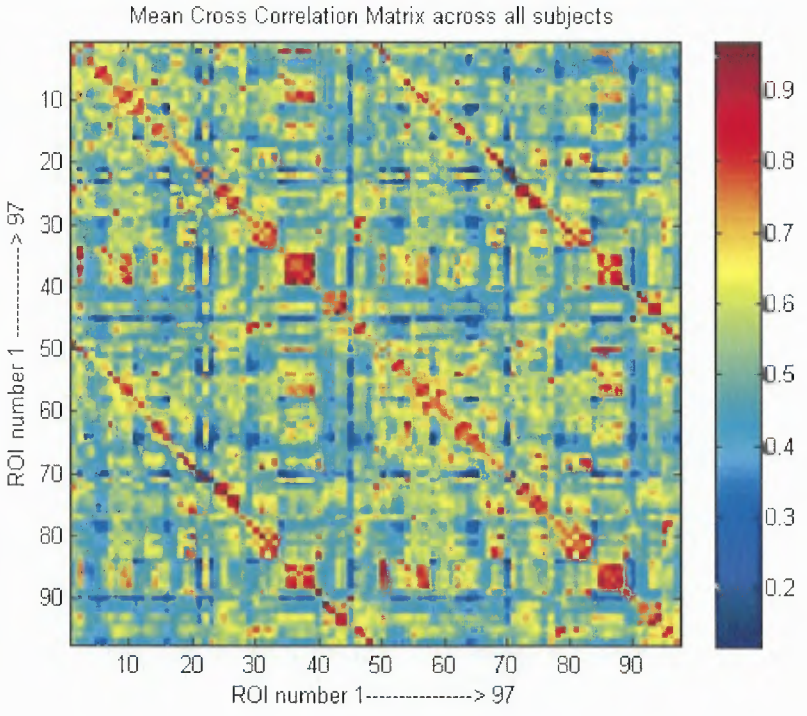


**Figure 4.4** Mean of Cross Correlation matrix for all subjects.

To further quantify results of reliability of these networks between sites scatter plot of mean cross correlation value of ROIs from one site versus the same ROIs from other site was drawn. Expected result of scatter plot was accumulation of points across diagonal rather than scattered around the plot because accumulation of points around

diagonal points out to similarities between mean cross correlations values of individual ROI pair.

Figure 4.5 shows scatter plot of mean cross –correlation value across all subjects versus mean of cross correlation matrix for an individual site. As discussed before accumulation of individual data points around diagonal in each of the scatter plot helps to strengthen the hypothesis by pointing at less variability between mean cross – correlation value of individual ROI pair for each site and mean cross-correlation value of that individual ROI pair across all subjects reducing possibility of an outlier.

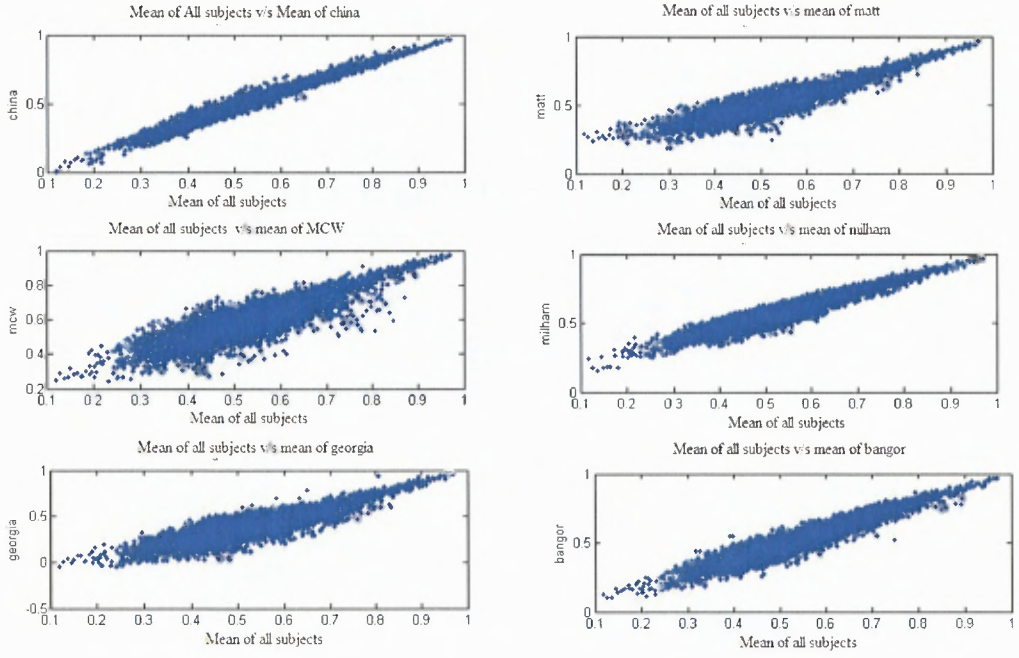


**Figure 4.5** Scatter plot of mean of cross correlation matrix for all subjects with all other sites.

Apart from comparison between mean of all subjects and mean of each site, checking reliability of resting state networks through comparison between mean cross-correlation values of ROI pair between sites. To check reliability of mean cross-correlation value of a ROI pair between sites, similar to previous step, scatter plot of

mean cross correlation value for each site with that of all other sites were drawn in expectancy to see similar results of clustering of data points around diagonal. Figure 4.6 shows scatter plot of mean cross correlation value of each ROI pair for china data with all other sites. As expected clustering of data points around the diagonal was observed confirming continuity of resting state network measures across sites. In Figure 4.6 the first figure is scatter plot of mean cross-correlation of chin dataset with itself making a single line at diagonal in order to make comparisons between scatter plots easy.

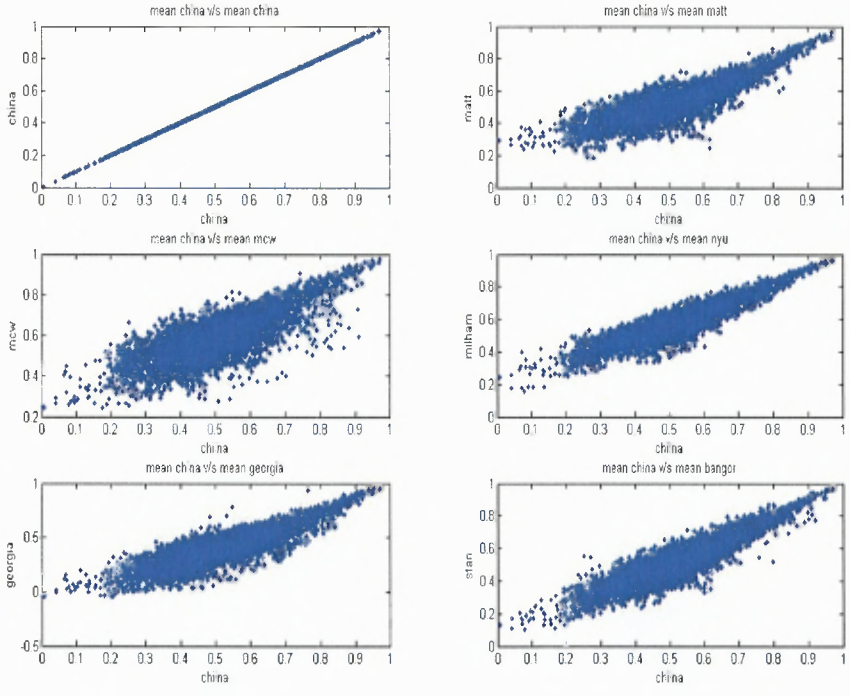


**Figure 4.6** Scatter plot of mean cross correlation matrix of all subjects of china dataset with all other sites.

Comparison between mean of cross correlation matrix between sites provides cost-efficient and primary way of checking reliability of resting state network but in addition to this it also makes results of mean-cross correlation value for ROI pair

susceptible to a possible outlier in any individual subject's data. A very high value of cross correlation for a ROI pair from an individual subject can give sudden rise to mean cross correlation of value of that ROI pair having otherwise low cross correlation value in a size having relatively lower number of subjects. To confirm consistency of resting state brain networks results from mean cross correlation value Principal Component Analysis was performed.

Principal Component Analysis is a very useful tool to determine principal components present in a large dataset. PCA can provide very good results with large dataset by reducing the data size to the number of principal components (having highest weight) in the dataset which can be very useful to reduce noise and reduce the data size to bare minimum. PCA works in similar manner as Fourier Transform reducing probability of effect of an possible outlier. In order to derive more reliable results of resting state brain networks measured by comparison of mean cross correlation value between sites and between individual sites with mean across all the sites PCA analysis using MATLAB 7.0 was applied to group cross-correlation matrix of all subject for each site and for all the subjects across sites. Out of the 20 principal components, output of PCA algorithm, first component was chosen as primary component.

Visual comparison between first PCA component of each of the dataset and mean of all the subjects showed very much similarity between them. Figure 4.7 and Figure 4.8 shows first PCA component of cross correlation matrix across subject for china dataset and first PCA component of cross correlation matrix across all subjects. Regional similarities between two are easily visible.

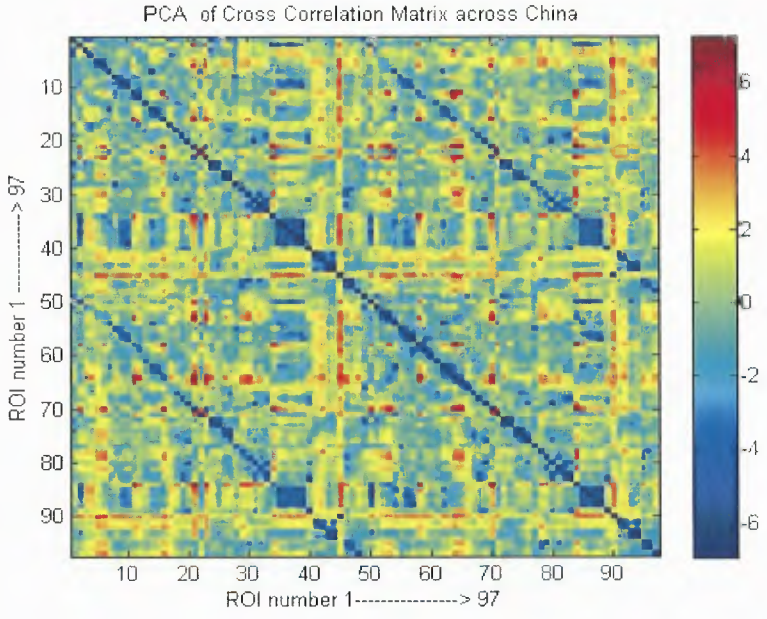


**Figure 4.7** First of PCA components for cross correlation matrix for China dataset.

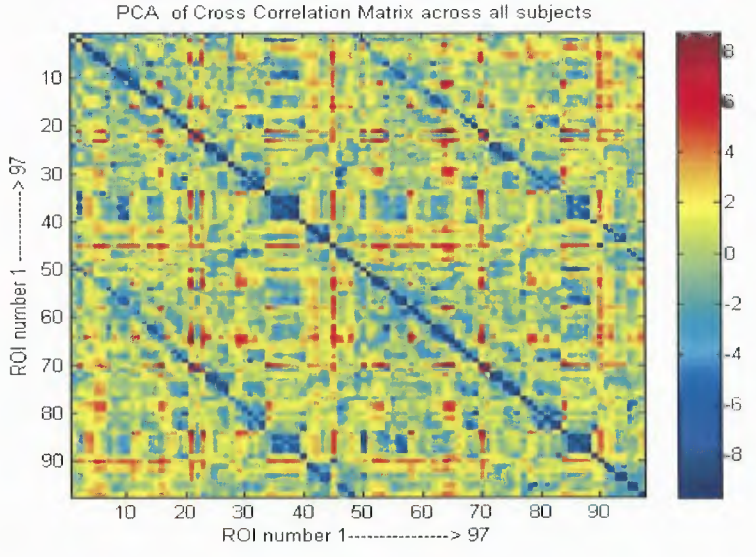


**Figure 4.8** First of PCA component of cross correlation matrix for all subjects.

Following the same procedure adopted for comparison between mean of cross correlation matrix between sites and between mean cross correlation of different sites and

mean across all subjects, scatter plots were drawn in order to compare first PCA component of cross correlation matrices for each site with each other and with first PCA component across all subjects. Figure 4.9 shows scatter plots of first PCA component across all subjects with first PCA component of each site.

As expected from the previous results accumulation of data points around diagonal in scatter plot suggests similarity between cross correlation values for a pair of ROIs between First PCA of components of all subjects versus that of each site.

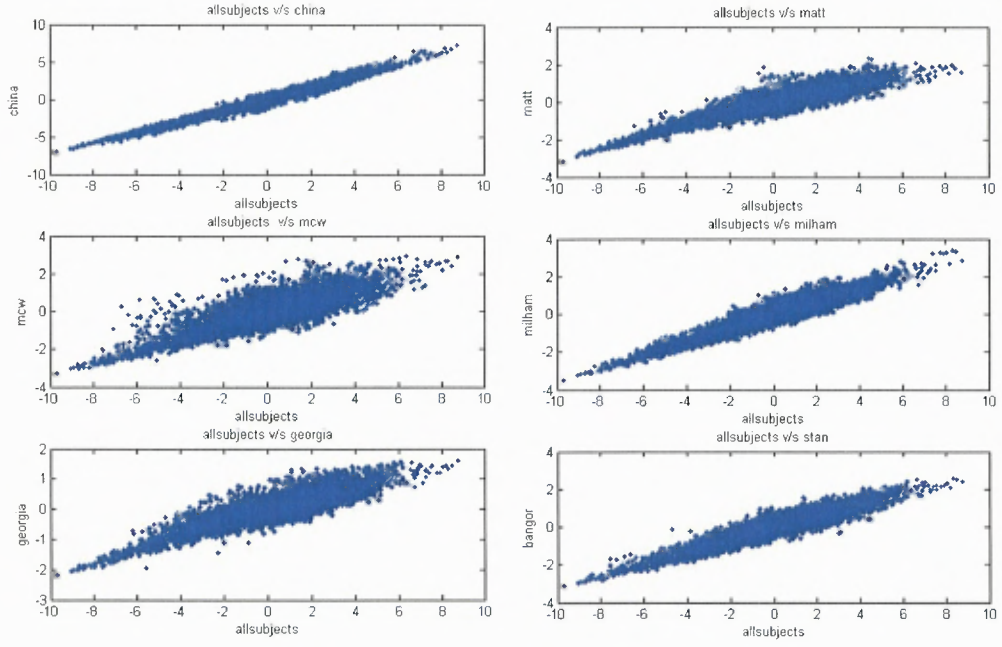


**Figure 4.9** Scatter plot of First PCA component of cross correlation matrices of all subject v/s first PCA component of cross correlation matrices for individual sites.

Figure 4.10 shows scatter plot of first PCA component of cross correlation matrix for china dataset with first PCA component of cross correlation matrix of all other sites showing same results as scatter plot of mean cross correlation matrix of china dataset with all other sites.

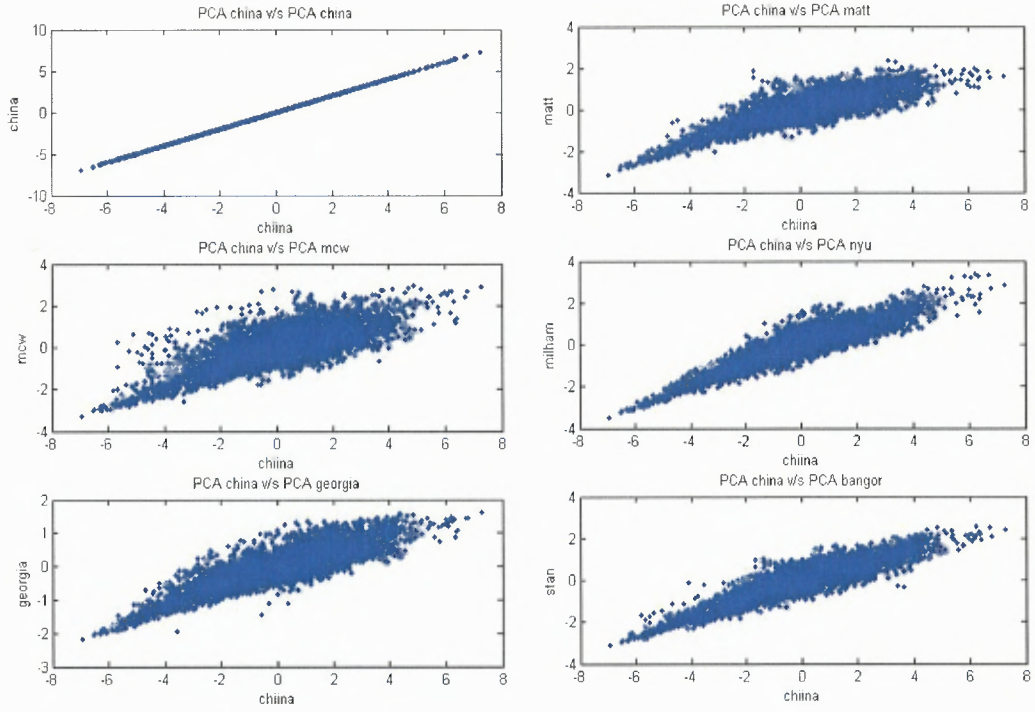


**Figure 4.10** Scatter Plot of first PCA component of cross correlation matrix for china dataset with first PCA component of cross correlation matrix for all sites.

# CHAPTER 5

# CONCLUSION AND FUTURE WORK

## 5.1 Conclusion

The primary finding of this study was that very robust intrinsic resting state functional connectivity was observed in a large set of subjects. This is one of the largest study to study resting state functional connectivity. In this chapter, the main finding of this study is presented along with shortcomings of this study. Also, directions into which investigation can be done have been proposed.

Very robust correlation structure was obtained across the majority of the more than 400 subjects used in this study. Further, strong correlation between regions was found across subjects. Similarly, weak correlation between ROIs remained consistent across subjects. Data used in this study, was collected across three continents. The robustness of the correlation structure represents an inherent intrinsic connectivity pattern present in the resting brain.

Resting state FMRI data of more than 400 subjects was acquired for this study. This is the largest study in fMRI showing minimal variation of results between subjects that were collected spanning three continents which show that even large groups of population can be used in fMRI and an epidemiology kind of study is possible. This may open new avenues into clinical research, where brain images can be used in conjunction with population based data.

The robustness of the resting state functional connectivity can be used in addition to the task activation paradigm. Resting state functional connectivity patterns may be used as an alternative to task activation studies. Further, in clinical cases including coma

and stroke where the subjects are not able to respond to tasks, resting state functional connectivity may provide as a viable alternative to study human brain function.

Primary limitation of this study is that because, the subjects did not perform any specific tasks, it is not possible to ascertain the underlying neural state of the brain. It is possible that the subjects were involved in imaging specific mental imagery that gave rise to correlation. This is however, not very likely scenario since it is highly improbable for all subjects to be imagining same kinds of thoughts.

This method was computationally expensive and required several hours to process each subject. Each of the processing step although was automated, a several steped, user verification was performed at the end to ensure that the various algorithms used converged in an optimal fashion for each of the subject. However, as more subjects are collected, scripting language, as was used in this study could be used to stream line the process saving development time to develop algorithm and more time can be spend on group comparison.

Although, each of the subjects was scanned during rest, various controls have still to done to facilitate proper collection of the data. For example, care has to be taken if the subjects had proper sleep the previous night, if they are hypoglycemic. In addition to these care needs to be taken to make sure that scanning parameters remains same across the sites to make measures more reliable and robust.

## 5.2 Future Work

This study provides a basic but well developed frame work for future studies to check reliability of resting state connectivity between pair of ROIs or on voxel vise studies. A few ideas are suggested to study reliability of resting state connectivity apart from comparison between cross correlation values between populations from three continents.

Recent studies have shown application of small world network properties on FMRI datasets to observe and derive structural connectivity pattern of brain regions based on functional responses of the brain regions rather than based on anatomical location of the region. These types of studies are done on very small scale of the data having minimal variation and related. Similar studies on large resting state FMRI dataset, similar to the one used in this study can provide more robust results about brains structural connectivity based on functional response. Comparison of results from such studies and previously established standards can also provide information about reliability and application of small world network studies to resting state FMRI data.

One important and interesting future work based on present study can be regarding study of effect processing strategy chosen on resting state measure. With such a large dataset a very little variation in processing parameters can provide a large difference in final result, not possible with studies of small dataset. Results of these types of studies can emphasis on determining of optimal processing strategy needed to be employed.

Application of granger causality statistics to ROI time series in resting state can provide information about probability measure of one ROI causing other during a rest scan. Established results from application of such studies to the dataset used in this work

can help to predict response and effect of an individual brain region during task paradigm.

## REFERENCE


1. Bandettini PA, Wong EC, Hinks RS, Tikofsky RS, Hyde JS. Time course EPI of human brain function during task activation. Magn Reson Med.1992;25:390-397.

2. Belliveau JW, Kennedy DN Jr, McKinstry RC, Buchbinder BR, Weisskoff RM, Cohen MS, Vevea JM, Brady TJ, Rosen BR. Functional mapping of the human visual cortex by magnetic resonance imaging. Science. 1991;254:716-719.

3. D. N. Kennedy , N. Lange, N. Makris , J. Bates, J. Meyer and,V. S. Caviness, Jr. Gyri of the Human Neocortex: AnMRI-based Analysis of Volume and Variance. Cerebral Cortex Jun 1998;8:372-384.

4. Ogawa S, Tank DW, Menon R, Ellermann JM, Kim SG, Merkle H, Ugurbil K. Intrinsic signal changes accompanying sensory stimulation: functional brain mapping with magnetic resonance imaging. Proc Natl Acad Sci U S A. 1992;89:5951-5955.

5. Biswal B; Yetkin F Z; Haughton V M; Hyde J S. Functional connectivity in the motor cortex of resting human brain using echo-planar MRI Magnetic resonance in medicine 1995;34(4):537-541.

6. Greicius M, Krasnow B, Reiss I, Menon V. Functional connectivity in the resting brain: a network analysis of the default mode hypothesis. Proc Nat Acad Sci USA. (2003);100:253-258.

7. Fox MD, Snyder AZ, Vincent JL, Corbetta M, Van Essen DC, Raichle ME. The human brain is intrinsically organized into dynamic, anticorrelated functional networks. Proc Nat Acad Sci USA. (2005);102:9673-9678.

8. Dosenbach NU, Fair DA, Miezin FM, Cohen AL, Wenger KK, Dosenbach RA, Fox MD, Snyder AZ, Vincent JL, Raichle ME, Schlaggar BL, Petersen SE. (2007). Distinct brain networks for adaptive and stable task control in humans. *PNAS* 2007 Jun 18.

9. Roberto Toro, Peter T. Fox ,TomaPaus. Functional Coactivation Map of the HumanBrain Cerebral Cereb Cortex. 2008 Nov; 18(11):2553-2559.

10. Shehzad Z, Kelly AM, Reiss PT, Gee DG, Gotimer K, Uddin LQ, Lee SH, Margulies DS, Roy AK, Biswal BB, Petkova E, Castellanos FX, Milham MP.Cereb Cortex. 2009 Feb 16.

11. William R.Hendee, E Russel Ritenour.Medical Imaging Physics. 4thed. Newyork: Wiley-Liss.2002.

12. Kumar A. Welti I Ernst R R.NMR Fourier zeugmatography.J. magnetic resonance, 1975; 18:69-83.

13. weng X dsing Y S ,volkowND ,IMAGING of the FUNCTIONAL HUMAN BRAIN ,PROC.NATL .ACAD SCI.USA 1999 ;12(5):11073-11074.

14. RW Cox. AFNI:Software for analysis and visualization of functional magnetic resonance neuroimages.Computers and Biomedical research;29:162-173,1996.

15. Friston, KJ Frith,CD Liddle,PF and Frickowiak,RS. Functional connectivity: the principal component analysis of large (PET) data sets.*J. Cereb. Blood. Flow Metab.* **13**, 5 (1993).

16. Hampson,M Peterson,BS Skuldarski,P Gore,JC. Changes in Functional Connectivity Using temporalcorrelations in MR images. Hum Brain Mapp. 15, 247 (2002).

17. Hampson,M Olson,IR Leung,HC Skuldarski,P Gore,JC. Changes in Functional Connectivity of human MT/V5 with visual motion input. Neuroreport. 7, 1315 (2004).

18. Xiong J, Parsons LM, Gao JH, Fox PT. Interregional connectivity to primary motor cortex revealed using MRI resting state images. Hum Brain Mapp.1999;8(2-3):151-156.

19. Skuldarski,P and Gore,JC. Changes in the correlations in the FMRI physiological fluctuations may reveal functional connectivity within the brain. *Neuroimage.* **3**, S600 (1998).

20. Lowe,MJ Davidson, RJ Orendi,J. Intra-hemispheric functional connectivity of FMRI physiological noise correlations: dependence on attention. *Proc.* 5th ISMRM, Vancouver, p. 1688 (1997b).

21. Biswal and J. S. Hyde. Functional connectivity during continuous task activation. *Proc.* 6th ISMRM, Sydney, p. 2132.

22. Hudetz, AG J. J. Smith, J. G. Lee, Z. J. Bosnjak, and J. P. Kampine. Modification of cerebral laser-doppler flow oscillations by halothane, PCO2, and nitric oxide syntahse blockade. *Am. J. Physiol.* ***269*** *(Heart Circl. Physiol.)* **38**, H114 (1995).

23. Biswal and J. S. Hyde. Functional connectivity during continuous task activation. *Proc.* 6th ISMRM, Sydney, p. 2132 (1998).

24. Biswal BB, Yetkin FZ, Ulmer JL, Haughton VM, Hyde JS. Detection of abnormal functional-connectivity in Tourette Syndrome using FMRI. Proc. 5$^{th}$ ISMRM, Vancouver, p 733(1997d).

25. Biswal BB, Hyde JS. Contour-based registration technique to differentiate between task-activated and head motion-induced signal variations in fMRI. Magn Reson Med. (1997e) 38(3):470-476.